

**NASA TECHNICAL  
MEMORANDUM**



NASA TM X- 52123

NASA TM X- 52123

GPO PRICE \$ \_\_\_\_\_

CSFTI PRICE(S) \$ \_\_\_\_\_

Hard copy (HC) \$3.00

Microfiche (MF) .50

ff 653 July 65

**FIBER-METAL COMPOSITES**

FACILITY FORM 602

**N65 35396**

(ACCESSION NUMBER)

**58**

(PAGES)

**TM X 52123**

(NASA CR OR TMX OR AD NUMBER)

(THRU)

**1**

(CODE)

**17**

(CATEGORY)

by J. W. Weeton and R. A. Signorelli  
Lewis Research Center  
Cleveland, Ohio

TECHNICAL PREPRINT prepared for Twelfth Sagamore  
Army Materials Research Conference sponsored by  
U.S. Army Materials Research Agency  
Raquett Lake, New York, August 24-27, 1965

NATIONAL AERONAUTICS AND SPACE ADMINISTRATION • WASHINGTON, D.C. • 1965

**FIBER-METAL COMPOSITES**

by J. W. Weeton and R. A. Signorelli

Lewis Research Center

Cleveland, Ohio

**TECHNICAL PREPRINT** prepared for

Twelfth Sagamore Army Materials Research Conference

sponsored by U.S. Army Materials Research Agency

Raquette Lake, New York, August 24-27, 1965

**NATIONAL AERONAUTICS AND SPACE ADMINISTRATION**

# FIBER-METAL COMPOSITES

by J. W. Weeton and R. A. Signorelli

Lewis Research Center  
National Aeronautics and Space Administration  
Cleveland, Ohio

## INTRODUCTION

E-5143

Although stronger and better conventional materials are always in the offing and always will be in demand, composite materials may offer the only hope of achieving certain space age requirements. Not only are unusual properties expected from such fiber bearing products, but it is expected that they may ultimately be made economically by mass production techniques. Design of composites utilizing the unique or unusual mechanical and physical properties of fibers would appear desirable. Beyond this, however, a more intriguing possibility exists; namely, that composites may evolve with time and considerable research and development effort and that they will have properties far better than would be expected from the individual properties of the constituents comprising the composites (a large synergistic effect). This paper is concerned largely with work that has been completed or that is underway at the NASA Lewis Research Center. An effort will be made, however, to review and present the work of others that pertains to some of the points that are to be made. This is particularly true in those cases where either fundamental concepts must be embellished or where outstanding high strength metallic matrix-composite materials have been produced by others. Consideration will be given to such fundamentals as fracture mechanisms and strength relationships. Some type of base line for comparison is needed to determine whether the composite equals or exceeds the potential expected based upon the properties of the fibers and matrix materials. Composite properties have been related to fiber and matrix properties utilizing a law-of-mixtures equation, that is, a principle of combined action. The law-of-mixtures relationship should be considered a "first approximation" because it is possible that the mechanical properties of the composite may be related to a host of metallurgical factors rather than the known strength of the constituents. Thus deviations from the law of mixtures may be related to such factors as relative strain hardening rates of matrices and fibers, relative moduli of elasticity, relative creep rates (for high temperature conditions), interfiber spacing, orientation effects, stress concentrations, and relative contraction of materials during elongation (Poisson ratio effects in tensile applications). Some of the factors causing deviations will also be discussed.

## LAW-OF-MIXTURES BEHAVIOR

This relationship was first shown to be valid for tensile strengths of metallic matrix systems in references 1 and 2, wherein a copper-matrix

was reinforced with tungsten fibers. Subsequently, the law-of-mixtures relationship was extended and shown to relate the yield strengths and the moduli of elasticity of volume percentages of fibers (using tungsten fibers embedded in a copper matrix) in the composite for both continuous and discontinuous specimens (ref. 3). A review of the work presented in references 1 to 3 will follow.

The studies were conducted at the Lewis Research Center. Composites consisted of tungsten fibers embedded in a copper matrix. This system was selected because copper and tungsten are mutually insoluble, because molten copper wets tungsten, because tungsten has a high recrystallization temperature, and because tungsten has a much greater strength and modulus than does copper. First, the case of continuous reinforcement will be considered, in which the fiber extends the full length of the test section.

Bundles of tungsten fibers were placed in a tube so that all the fibers were oriented in a direction parallel to the tensile axis. The wires were infiltrated with molten copper. Infiltration was carried out in various atmospheres including vacuum and hydrogen. The cross section of a typical specimen is shown in figure 1. The strength of such composites were found to be represented by the following equation:

$$\sigma_c = \sigma_f A_f + \sigma_m^* A_m \quad (1)$$

where

$\sigma$  ultimate tensile strength

$A$  area fraction or volume fraction when unity length is considered and

$$A_f + A_m = A_c = 1$$

$\sigma_m^*$  stress on matrix, taken from stress-strain curve, at equivalent strain to that at which ultimate tensile strength of fiber is achieved

and the subscripts are

$c$  composite

$f$  fiber

$m$  matrix

Figure 2 shows some typical stress-strain curves for tungsten, copper, and tungsten-fiber-reinforced copper composites. It may be seen that the copper carries only a minor stress (8000 psi) compared with the tungsten fiber, which carries over 300,000 pounds per square inch. Figure 3 shows a plot of ultimate tensile strength versus volume percent of tungsten fiber for 5-mil tungsten-fiber-reinforced copper composites. Similar curves were obtained for 3- and 7-mil-diameter wires, and all of these data are discussed in more detail in reference 3. The straight line of figure 3 extends from



the tensile strengths of the tungsten fibers (thermally treated to duplicate the treatment given the fibers by the infiltration process used) to the stress carried by the copper matrix. Note, however, that the copper stress used is the stress on the matrix, taken from the stress-strain curve, at an equivalent strain to that at which the ultimate tensile strength of the fiber was achieved. (See the definitions given for eq. (1).) The dashed portion of the curve at the left indicates the range of volume percent fiber content over which the fiber does not contribute to the tensile strength of the composite. The fiber breaks before the maximum load of the composite is reached. The intersection of the dashed line and the solid line may be termed the critical volume percent and is defined as the lowest volume percent fiber content where fibers break as the maximum load carrying capacity of the composite is reached. Thus the tensile-strength - law-of-mixtures relationship does not apply to composites containing volume percentages of fibers below the critical percentages. Another point could be made from this figure; namely, that some of the composite materials are very strong. For example, at 50 volume percent of fibers, the tensile strength of the composite is over 150,000 pounds per square inch. At 75 percent, the strengths are over 250,000 pounds per square inch.

Figure 4 shows the same curve obtained previously both experimentally and by calculation using equation (1) for the continuous fibers. However, the data points on this curve represent ultimate tensile strengths obtained from composites reinforced with discontinuous fibers. In these composites, fibers were cut into 3/8-inch lengths. They were oriented in the direction of the specimen axis and infiltrated in the same manner as was done for the full-length fibers. Composite specimens containing a maximum of 41 volume percent fibers were made by this method. The data points fell fairly close to the previously obtained curve. This, of course, was very encouraging because it permitted a prediction that discontinuous, or short-length fibers, such as whiskers or other strong materials, could be embedded in the matrix materials and be expected to contribute significantly to the strength of the composite. In fact, for many practical composites, ultimately to be made, strengths obtainable for specimens with relatively short fibers are expected to be within experimental accuracy of those obtained for continuous fibers.

Figure 5 shows the four stages of stress-strain behavior of the composites during tensile testing. Evidence was presented in reference 3 to indicate that such behavior occurred in the tungsten-fiber - copper-matrix materials. For very low percentages of strain, both the fiber and the matrix would be elastic (stage I). As the material would be strained further, the fiber would still be elastic and the matrix would become plastic (stage II); continuing to elongate the composite, the fibers then become plastic and the matrix remains plastic (stage III). At some point the fibers would begin to break (stage IV). The fact that composite curves did not fall off in strength very rapidly indicated that the segments of the fibers that had fractured were still retained and bonded to the matrix and reinforced the material by acting as short-length fibers.

Some of the experimental work, which indicated that the composites had four stages of behavior, as indicated in figure 5, are presented in figures 6 to 8. Figure 6 shows the dynamic modulus of elasticity obtained by sonic techniques. The results represent stage I behavior and is the initial modulus of elasticity of the composites reinforced with either continuous or discontinuous fibers. The linear relationship between the modulus of the composite and the volume fraction of the fibers is, of course, a law-of-mixtures relationship.

In considering Stage II behavior, it is necessary to examine the stress-strain curves of the composites in stage II and their component phases at strains larger than those representing only the elastic behavior of the least elastic component. It was shown that the copper stress-strain curve deviates from proportionality at about 0.03 percent strain. Above this strain, copper deforms plastically and exhibits an almost flat or horizontal stress-strain curve. The slope of the composites were shown to decrease in going from the first linear slope in this strain-region of stress-strain curves to the second almost linear region at somewhat higher strains. A linear secondary slope would not be expected for a composite with a matrix that did not exhibit a linear stress-strain curve in the region of plastic strain of the matrix. This portion of the curve on the schematic diagram (fig. 5) is termed secondary modulus of elasticity. Again, as was the case for the initial modulus curve, the secondary modulus of elasticity obeyed a linear relationship with fiber content (fig. 7). These values were measured with extensometers. At zero volume percent fibers, the curve extrapolated to a value equal to the approximate slope of the plastic portion of the stress-strain curve of copper. At 100 percent fiber content, the curve extrapolated to a value equal to the modulus of elasticity of tungsten. This indicated that the matrix was plastic and the fiber elastic in stage II.

As the composite was strained further, the fiber also became plastic (stage III). Figure 8 shows the yield strengths obtained from the stage III portion of the stress-strain curves of the composites. The stress at 0.2 percent offset was determined by drawing a line parallel to that portion of the curve where the fibers were elastic and the matrix was plastic (stage II portion of curves). Again, the data points fall on a straight line, and the curve extends from the yield strength of the copper to the yield strength of the tungsten. Thus, yield strengths also obeyed a law-of-mixtures relationship.

It is evident by inspection of the stress-strain curves of the composite specimens of figure 2 that with continuing strain the composites reach their ultimate strength. After the attainment of the ultimate strength, some fibers fracture within the composite (stage IV). The fracturing of all the fibers in a composite would not be expected to occur simultaneously; with additional strain of the composite, other fibers fracture at random locations along their length. Figure 9 shows cracks that formed in fibers some distance away from the main fracture. Such fractures would occur after the ultimate strength of the composite was obtained, but before the final fracture of the specimen occurred. The segments of the fractured fibers retained

their bond with the matrix and acted as short-length fibers reinforcing the composite. The latter is believed to be the case because the composite stress-strain curves were very flat or tapered off in strength slowly relative to the stress-strain curves for the tungsten fibers alone, indicating that the reinforcing was continued by the fiber segments. Elongation of the composites was greater than that of the fibers tested individually.

In composite specimens, load is transferred from fiber to fiber by shear through the matrix. The area of matrix fiber interface available for load transfer with discontinuous fibers is reduced compared with that of continuous fibers. Therefore, care must be taken to prevent shear failure of the matrix or matrix-fiber interface rather than tensile fracture of fibers. The shear transfer of loads has been described previously for metallic composites (refs. 1 to 3) and for glass-reinforced plastics (ref. 4). A schematic model is shown in figure 10. The discontinuous fibers in the composite are aligned parallel to each other and to the tensile axis. It is assumed that the fibers overlap each other by varying amounts and that they are individually bonded to the matrix. Using this model, the value of  $L/D$  or the aspect ratio necessary to fully utilize fiber strength, was shown to be represented by the equation

$$\frac{L}{D} = \frac{1}{4} \frac{\sigma_f}{\tau} \quad (2)$$

where

- L length of fiber overlap needed to transmit shear stress equal to tensile stress on fiber
- D diameter of fiber
- $\sigma_f$  tensile strength of fiber
- $\tau$  shear strength of fiber-matrix interfacial bond or shear strength of matrix, whichever is less

When the entire fiber is embedded in the matrix, the required fiber length would be twice the value of  $L$  given above or

$$\frac{L_c}{D} = \frac{1}{2} \frac{\sigma_f}{\tau} \quad (3)$$

where  $L_c$  is the total fiber length; the minimum fiber length needed to permit the fiber to contribute its tensile strength to the matrix by shear. The other terms are the same as those noted for equation (2). (See fig. 11 for schematic illustration.) The midportion of figure 11 shows a schematic illustration of the tensile stress distribution along a fiber of critical length embedded in the matrix. This is the shortest length fiber that permits a stress buildup within the fiber to cause tensile fracture. The average stress on a fiber of critical length is also illustrated and is

equal to one half of the stress carrying capacity of the fiber material. This, of course, assumes that the buildup of stress from the end of the fiber to the center is linear. The bottom portion of the figure shows a fiber that is much greater than the critical length and also illustrates how this affects the average stress carrying capacity of the fiber. Again the stress is assumed to buildup linearly from each end to the value to cause tensile fracture of the fiber, but now a greater proportion of the fiber can carry the full tensile load. Thus, the average stress on the fiber is considerably higher than the average stress on a fiber of critical length and, in fact, may approach the average stress of the continuous fiber.

Kelly and Tyson (ref. 5) derived a modified law-of-mixtures equation that showed the relationship between strength of discontinuous-fiber composites and fiber lengths. It should be remembered that the fiber length also bears a relationship to the aspect ratio and thus the equation shows the importance of length and/or aspect ratio. The equation is as follows:

$$\sigma_c = \sigma_f V_f \left(1 - \frac{1}{2\alpha}\right) + \sigma'_m (1 - V_f) \quad (4)$$

where

$\sigma$             tensile strength

$V_f$            volume fraction of fibers or same as  $A_f$  of eq. (1)

$\alpha$             actual fiber length/critical fiber length,  $L/L_c$

$\sigma'$            same as that for  $\sigma^*$  of eq. (1)

$1 - V_f$        $V_m$ , volume fraction of matrix or  $A_m$  of eq. (1)

$L$             actual fiber length

$L_c$            fiber length needed to permit fiber to contribute its tensile strength to composite, that is, critical fiber length

Equation (4) indicates that discontinuous length fibers will not contribute 100 percent of their strength to the composite. On the other hand, with lengths many times the critical length (large aspect ratios) the values calculated are effectively the equivalent of values obtained with continuous fibers (eq. (1)). For example, with  $L/L_c = 10$ , 95 percent of fiber strength would be contributed; with an  $L/L_c = 100$ , 99.5 percent of the fiber strength could be utilized. It is believed that it will prove relatively easy to produce composites with fibers having  $L/L_c$  values such that better than 90 percent of the fiber strengths will be usable.

Values of the critical length or length-to-diameter ratio were found experimentally by determining the maximum length of a fiber that can be pulled out of the matrix (ref. 6). Such a procedure would seem to give a

very direct method for determination of the critical length-to-diameter ratio. Results of such an experiment are shown in figure 12. Here the stress required either to break the wire or to pull it from a piece of copper is plotted as a function of twice the length of the portion embedded in the matrix divided by the diameter. The point at which the curve of figure 12 bends over and becomes horizontal is the critical length-to-diameter ratio since this is a point at which the shear strength of the matrix or of the interface is equal to the strength of the fiber. When this length is exceeded, the fiber fractures.

Kelly and Tyson obtained curves such as those shown in figure 13 for specimens tested at different temperatures and for different sizes of wires. Utilizing the slopes of such curves and the  $L/D$  ratios, the critical length-to-diameter ratios were calculated. They were able to show not only the effects of increasing temperature upon the critical length-to-diameter ratio but also the effects of temperature on the shear strength of the matrix at the fiber-matrix interface. The latter was possible with the utilization of equation (3) and the obtained critical length-to-diameter ratios. The calculated shear strengths decreased with increasing temperature, as would be expected, and the need for the utilization of larger length-to-diameter ratios at elevated temperatures was made evident. The fiber tensile strength and the matrix shear strength both decreased with increasing temperature. However, the copper shear strength decreased at a much higher rate. This would be expected since the copper is at a much higher fraction of its melting point. Thus, matrix strength plays the predominant role in determination of required  $L/D$  values for the tungsten fiber-copper composites. These composites may be representative of high melting-point fibers embedded in low melting-point matrices.

#### DEVIATIONS FROM LAW-OF-MIXTURES BEHAVIOR

Some of the factors or phenomena that could conceivably produce synergistic effects in a composite (in this case, properties greater than those predictable from law-of-mixtures calculations) are the following: alloying reactions at the fiber-matrix interface, surface strengthening of the fiber within the matrix by healing or elimination of surface defects, size effects, crack interruption, dissipation of stresses at crack apex by ductile matrix, blockage of cracks by strong fibers, orientation of grains at surfaces of fibers, orientation of grains throughout fiber, restraint and constraint of fiber deformation by matrix, restraint and constraint of matrix by fiber, thermal expansion effects, corrosion prevention by matrix, and probably numerous other effects.

Very little published data exists to date that indicates synergistic effects may be obtained by combining fibers in metallic matrices. An example of possible improvements in composite strengths above law-of-mixtures values has been published by Piehler (ref. 7). The composites made by Piehler consisted of steel fibers (0.8 percent C Piano wire) embedded in silver. Full-length fibers, either 7 or 19 per cross section, plated with varying thicknesses of silver, were packed together

in a hexagonal stacking pattern in a silver tube and consolidated by a combined mechanical working and heat treating procedure. Figure 14 shows the tensile strength of composites made by this method on a strength versus volume percent basis. It may be seen that the tensile strength of the composites fall above the line drawn between the tensile strength of pure silver and the tensile strength of fibers (fibers were dissolved from composites for tests). The author attributed the higher strength of the composites, relative to the law-of-mixtures line, to constraint and restraint factors, in particular to the restraining of localized necking of fibers by the matrix.

It should be mentioned, however, that it is possible that metallurgical factors, other than restraint, could have accounted for the apparent increase in properties above the law-of-mixtures values. It is felt that there is a possibility that the materials used to represent the matrix and fiber strengths were not representative of their counterparts within the composite.

One of the major considerations relative to the successful fabrication and use of composites is that of the compatibility of materials. It has been mentioned that alloying and other metallurgical reactions between fibers and matrix materials within composites during fabrication and use may improve properties of constituents within the composites and concurrently cause the composite as a whole to be improved above expected values. Unfortunately, the converse possibility also exists, namely that reactions between materials can be deleterious.

Between the extreme possible effects noted above, that is, either large synergistic reactions or catastrophic damage, there may be varying degrees of improvement or damage to composite properties. For example, where mutually insoluble materials are combined there may be no reactions or loss or gain of strength resulting from the combinations. Even where alloying effects or reactions take place, the reactions may be controllable and resulting composites may have highly desirable properties.

At this time, no known evidence has been presented in the literature to indicate that the first effects noted above have been obtained from alloying reactions occurring in composites. As the second consideration, relatively few metal fiber-metal matrix systems exist that would permit the creation of composites consisting of nonreactive materials such as mutually insoluble constituents. Ceramic-fiber-metal systems would, in many cases, be expected to be relatively nonreactive. On the other hand, it is known that under some conditions even the most thermodynamically stable oxides may dissolve in metal matrices. In whisker bearing composites, too, reactivity between whiskers and metal matrices could also prove deleterious.

Further, it is almost a certainty that some of the most intriguing combinations of materials (from a potential strength standpoint) will prove most difficult to combine without having harmful reactions. Rather than attempt to predict such problems, investigations that have already been completed will be described. The problems encountered and some readily

observable effects of reactions upon fiber composite strengths will be made evident.

The first investigation concerned with compatability problems that will be described was conducted at the NASA Lewis Research Center. The principal objective was to obtain an understanding of some of the effects of alloying on the tensile properties of composites (ref. 8). It should be recalled that initial work described earlier was conducted with the tungsten-fiber - copper-matrix system, and that these materials are mutually insoluble (nonreactive). Alloying elements with varying degrees of solubility in tungsten were added to copper, and the resulting alloy was infiltrated about bundles of tungsten fibers. The infiltration conditions were the same as were used for the previous work (ref. 3). Room temperature tensile tests were made of the composites and a metallographic study of the microstructure of the fiber-metal matrix interface was conducted. The results were compared with those obtained in reference 3 in which copper was used as the matrix.

The tensile strength of some of the composites investigated is plotted against the volume percent fiber content in figures 15 and 16.

Three types of reaction were found to occur at the fiber-matrix interfaces within the composites. The reactions that formed are believed to account for the properties of the materials presented in the figures. The reactions included (1) a diffusion-penetration reaction accompanied by a recrystallization of the grains at the periphery of the tungsten fibers, (2) a precipitation of a second phase in the binder materials near the periphery of the fiber, which did not cause recrystallization of the fiber, and (3) a solid solution reaction, which did not cause recrystallization in the fiber. The resulting reactions that occurred at the fiber-matrix interface are also indicated. It can be seen that the tensile strength of the alloyed composites were all lower than that obtained for copper composites in which alloying with the fiber did not occur. With 5 percent nickel added to the copper, very little damage was done to the strengths of the composites. With 10 percent nickel, a considerable reduction in tensile strength was observed. Thus, it is evident that the percent of alloying additives to a matrix material may produce drastic differences in the properties of the composites. The most damaging type of reaction observed was the diffusion-penetration reaction accompanied by recrystallization of the fiber, which occurred with the copper-nickel and copper-cobalt matrix composites.

Figure 15 also shows the effects of adding 10 percent zirconium to the matrix of various composites. There is some reduction in the strength of the material, but again as was the case for 5 percent nickel additives the damage was relatively slight. In the case of the data point representing the 33 percent zirconium addition, there was a significant lowering of the tensile strength of the composite relative to the tensile strength of the pure copper-tungsten composites. This was attributed to the brittle nature of the matrix itself rather than to any alloying reaction

between the matrix additive (zirconium) and the tungsten fiber.

Figure 16 shows a strength-composition diagram for copper-tungsten composites to which small percentages of chromium or columbium were added. These elements form solid solutions with tungsten, and it was not possible to add larger percentages of these materials without raising the melting point above 2200° F. All of the data points for these materials fall very close to the line obtained for the pure tungsten-copper composites.

The microstructures of cross sections of some of the composites studied are shown in figures 17 and 18. The 5 percent nickel addition to copper did not cause the formation of a visible reaction zone (recrystallization zone) at the fiber-matrix interface (fig. 17(a)). The microstructure of this specimen is identical in appearance to one that would be obtained if pure copper were the matrix. The 10 percent addition of nickel, however, formed a large reaction zone (recrystallized zone) at the periphery of the fiber (fig. 17(b)).

Tensile strengths of the copper-5 percent nickel composites were much higher than those obtained for the copper-10 percent nickel composites and were only slightly lower than strengths of the copper composites. The lower tensile strength values for the copper-10 percent composites was attributed to the reaction zone formed with the fiber. As the depth of penetration or size of the reaction zone increased the tensile strength of the copper-10 percent nickel composites were found to decrease.

Figures 17(c) and (d) show the formation of recrystallized zones as a result of small additions of cobalt to copper. As little as 1 percent cobalt additions to copper recrystallized the tungsten fiber. The composites also were found to have tensile strengths much lower than that obtained for the pure copper matrix composites. It was also found that, as the depth of penetration of the alloying element into the tungsten fiber increased, the tensile strength and ductility decreased. It was shown for the copper-5 percent cobalt system that low tensile strength and poor ductility were not solely due to the contribution of the alloy zone formed with the fiber but also were due to the brittle nature of this zone and its effect upon the unalloyed portion of the fiber. Since recrystallized tungsten wire is extremely brittle at room temperature, the recrystallized zone of the fiber was believed to act as a brittle skin. It was felt that the recrystallized zone fractured or cracked early in the tensile test and that the crack acted as a circumferential notch around the fiber. Since tungsten is known to be notch sensitive, the formation of a notch by the brittle alloy zone would cause premature failure of the unalloyed portion of the fiber. Fibers that are notch sensitive might thus be readily damaged by alloying reactions at the interface between the fiber and the matrix. These conclusions or postulates were made with the aid of the plot shown in figure 19. The graph gives values for fiber tensile strengths (for fibers embedded in a copper-5 percent cobalt alloy matrix) obtained from graphical extrapolations of composite data as a function of the recrystallized



area of the fiber. Relative brittleness of the various composite fractures (also fiber brittleness) are indicated in the figure also. As the percentage of the recrystallized fiber zone increases (i.e., as depth of recrystallization increases), the fiber strength decreased. More important though, at a given point (about 30 percent recrystallization) the properties fell off at a rate greater than that which would be expected if the damage to the strength of the fiber were in direct proportion to the area of recrystallization. This, coupled with the change in ductility of the fractures, indicated that the fiber core which was recrystallized was being notch sensitized during the tensile test as was noted above.

Since many metallic fibers gain a considerable portion of their strength from mechanical deformation processes or from heat treatments both of which impart considerable strain energy to the material, it would not be surprising if, during incorporation of such fibers into a matrix, properties of the fibers were reduced. A reduction in properties could result from thermal or mechanical treatments used to fabricate the composites as well as by alloying reactions. The findings of this paper were encouraging to the authors in that they showed that very highly stressed fibers would not necessarily be severely damaged by alloying reactions. Although all of the alloying additions made to the matrix lowered the strengths of the composites, some alloying elements did no more than superficial damage to the fibers at temperatures at which other elements did severe damage to the fibers.

The work of Cratchley (ref. 9) will show some interesting strength-to-aspect ratio relationships and a law-of-mixtures behavior. The composite of interest is a stainless-steel fiber-reinforced aluminum-matrix material.

A solid-state sintering method was used to fabricate the composites. The temperature utilized ( $550^{\circ}\text{C}$ ) was low enough to minimize reaction at the fiber-matrix interface. Wires, 2 and 5 mils in diameter and  $1/4$ ,  $1/2$ , 1, and 2 inches in length were used. The composites ranged from short-length fiber reinforced composites to full-length fiber composites.

Figure 20 shows a plot of the tensile strength against the volume percents of fibers for one of the types of composites made by Cratchley. The fibers in this case were 2-mil fibers that were  $1/2$  inch long. The stainless steel contained 18 percent chromium, 9 percent nickel, and 0.6 percent titanium. The volume percentages of fibers in these composites ranged from approximately 6 to 14. It should be pointed out that it is difficult to incorporate large volume percentages of short-length fibers in the matrix, as may be recalled from the work that was done in references 1 to 3. An extrapolation of the curve presented by Cratchley would extend to a value of tensile strength almost exactly equivalent to the strengths of the fibers that he utilized (fig. 20). The data then appeared to obey a law-of-mixtures relationship. This was true even though there may have been a very minor reaction at the interface between the fiber and the matrix. The procedures utilized, however, eliminated deleterious effects from an interface reaction if there were any.

Cratchley also showed some of the effects of differing aspect ratio upon the strength of composites. Figure 21 shows a plot of the tensile strength against volume percent of composites containing fibers of different length-to-diameter ratios. With an aspect ratio of 830, the extrapolated strength of the fiber was approximately equal to the known strength of the fiber as determined individually, which would indicate that this material was essentially obeying a law-of-mixtures relationship. Cratchley also observed that decreasing fiber diameter increased the efficiency of reinforcement for a given fiber length.

## HIGH TEMPERATURE STRENGTHS OF FIBER COMPOSITES

Most of the research and development programs relating to fiber-reinforced metal composites have been concerned with short time, low temperature properties. It will be shown in the ensuing section that the elevated temperature potential of fiber-reinforced metal composites should be most exciting to the high temperature metallurgist for both short and long time applications.

### Tensile Strengths of Composites at Elevated Temperatures

An understanding of the strengthening mechanisms for fiber reinforcement at elevated temperatures was felt to be a requisite to permit the design of "high-temperature" composites. To gain an insight into the high temperature behavior of materials, a tungsten-fiber - copper-matrix model system (mutually insoluble materials) was again used as a basis for comparison (ref. 10). Fibers extended the full length of the specimens and were uniaxially oriented. In addition, tungsten fibers were also embedded in matrices of copper-2 percent chromium and copper-10 percent nickel alloys. Tensile tests were run at temperatures ranging from room temperature to 1800° F. Previous studies described earlier (see also ref. 8) had indicated that chromium, which formed a solid solution at the tungsten-matrix interface, did not reduce room temperature tensile properties significantly. Nickel, in the copper-base matrix, on the other hand, severely damaged the fibers by causing recrystallization. A comparison of the properties at elevated temperatures with previously obtained room temperature results would permit not only a comparison of behavior of a mutually insoluble materials system but systems with "damaging" and "nondamaging" reactions.

Elevated and room temperature tensile test results for the materials tested at temperatures of 300°, 600°, 900°, 1200°, 1500°, and 1800° F are presented in figures 22 to 24. Figure 22, which represented tungsten fibers in a pure copper matrix indicates that, for temperatures up to 1200° F, the law-of-mixtures relationship has been observed. Individual fiber strengths were difficult to obtain accurately at temperatures above 1200° F because of difficulties in controlling the test apparatus atmosphere. Therefore no data are shown for the fiber strengths at 1500° and 1800° F.

Presumably, the "straight-line" of the figures would extrapolate to the fiber strengths at these temperatures, also. Figure 23 gives test results for both tungsten-fiber-reinforced copper (dashed line) and the tungsten-fiber-reinforced copper-2 percent chromium alloy (solid line). The curves for the specimens tested at room temperature with the alloy matrix are almost identical with the curve for the pure copper-tungsten composite. It is very interesting then to notice that, at elevated temperatures too, the composite strengths fall almost on the law-of-mixtures curve for the pure copper-tungsten composite. The fiber strengths that are given in figure 23 are obtained from specimens digested from the copper-chromium matrix. The diameters of these fibers increased slightly as a result of the diffusion of chromium into the fiber and the formation of a chromium rich layer at the fiber periphery. Dissolving the matrix did no noticeable damage to the fibers that were embedded in the copper-chromium alloy matrix.

A contrasting picture from that noted above for chromium was obtained with the tungsten fibers embedded in the copper-10 percent nickel matrix (fig. 24). First, at room temperature, as was noted in the earlier studies, the strengths of the copper-nickel matrix - tungsten-fiber composites were much lower than the strengths of the pure copper-tungsten composites (fig. 24). However, when the temperature was raised to 300° F (fig. 24) the tensile strengths of the composites were increased relative to the room temperature strengths (fig. 24). Presumably, the test temperatures above 300° F were above the brittle-to-ductile transition temperature of the fibers. Unlike the situation that existed for the chromium bearing matrix composites, the copper-nickel-tungsten fiber composites were appreciably weaker than the copper-tungsten fiber composites at all test temperatures. Attempts to obtain the strength of the tungsten fibers (with the recrystallized zone resulting from the nickel) by dissolving the matrix and extracting and testing the fibers failed. The fibers were so brittle that they failed in handling, actually shattering in most cases. Extrapolation of the composite strength versus volume percent fiber curves presumably would give both the strength of the matrices of the composites as well as the strengths of the fibers.

Figure 25 summarizes the strengths against test temperatures for fiber specimens, for 70 percent fiber composite specimens of the copper-tungsten composites, for the copper-2 percent chromium-tungsten fiber composites, and for the copper-10 percent nickel-tungsten fiber composites.

The importance of the shear strength of the matrix has previously been shown for discontinuous fiber composites tested at room temperature. Since the strength of the matrix may decrease rapidly with increasing temperature, the need to provide adequate shear length of the fiber-matrix interface becomes more acute as the temperature is raised. The drastically reduced fiber length necessary at elevated temperatures to prevent pull-out of fibers from the matrix may be seen in figure 26. The figure also shows the minimum  $L/D$  necessary to avoid pull-out of a tungsten fiber from a copper matrix for a range of temperatures (ref. 6).

In addition, it will be shown that a misalignment of fibers is a further source of concern with discontinuous fiber-reinforced composites, particularly, in those cases where the matrix is weak. Effects of fiber length and orientation on the elevated temperature tensile behavior of discontinuous tungsten fiber-reinforced copper composites are being studied at the Lewis Research Center (ref. 11). The effects of decreasing the fiber length on tensile properties that have been determined to date are shown in figure 27. Plots of tensile strengths for continuous and discontinuous fibers with an  $L/D$  ratio of 200 and 100 are shown. The curves are calculated using equation (4), which assumes perfect axial alignment of fibers. Comparison of the curves shows an expected decrease in efficiency of reinforcement with decreasing length of fiber. In the case of the specimens with an  $L/D = 200$ , the data points fall fairly close to the calculated curve. In the specimens containing fibers with an  $L/D = 100$ , there is a considerable scatter of data with several points well below the calculated line. It is believed that the lower strengths resulted from an increased misalignment that might be expected with shorter fibers. A correlation of the low strengths with misalignment was obtained by an examination of the failed specimens. Figure 28 shows a specimen with alignment adequate enough to cause tensile failure of the specimen. Also shown is a specimen where misalignment caused a shear failure of the matrix. Figure 29 is a schematic showing how the stress on a composite may vary with the orientation of the fibers. It also illustrates the failure modes that would be expected for different orientations of fibers. This figure was constructed from the equations of Stowell and Liu (ref. 12), which were also presented by Kelly and Davies (ref. 13).

For a small misalignment of the fibers from the axial direction the tensile strength increases slightly. This increase results from the fact that the fibers are oriented in a direction that requires a greater force than the axial stress, (i.e., to the fibers) to fracture them. Also, the matrix between the fibers is oriented in such a manner that it is strong enough to support a shear load capable of fracturing the fibers in the direction of the orientation. Further misorientational leads to shear failure of the matrix, which is indicated by the drop in the curve with increasing misorientation. A shear failure was pictorially shown in figure 28. It would be expected that at  $45^\circ$  the resolved shear stress would be a maximum and the composite stress would be a minimum. As the angle is increased above  $45^\circ$ , there is a tendency to stress the matrix alone in tension rather than shear, which would cause tensile failure of the matrix.

#### Stress-Rupture Strength

When it comes to creep or stress-rupture properties, there are almost no data available for fibers. Paradoxically, some of the most immediate foreseeable applications of fiber-reinforced materials are for aerospace turbine materials with attractive high temperature creep-rupture properties, rather than for high temperature, high tensile strength

materials. Since creep is an elongation process at a much slower rate than that which occurs during a tensile test, some similarities in the behavior of a fiber composite under creep conditions to the behavior under tensile conditions might be expected. On the other hand, the constant loading during rupture tests is different from the steadily increasing load conditions of a tensile test.

To gain an insight into the behaviors of such composites, it was felt that the strengthening mechanisms associated with the reinforcement of metallic matrices by fibers for creep-rupture conditions should be studied. The program at the Lewis research Center was expanded to include an investigation of stress-rupture behavior of tungsten reinforced copper composites. The rupture work has been conducted on tungsten reinforced copper composites at 1500° F. Fibers were continuous and uniaxially oriented. It should be emphasized that although this work is just beginning, the results seemed significant enough to describe at this time. Furthermore, a discussion of this work will complete the summary of the "model" or mechanism studies that have been conducted at the Lewis Research Center.

Tungsten-fiber-reinforced copper composites were stress-rupture tested at a temperature of 1500° F (~0.8 mp of Cu). Figure 30 shows some cross plots of data very recently obtained for full-length, fiber composites uniaxially oriented (ref. 14). The solid portions of the curves in this figure are cross plots representing the volume percent of fibers studied and the stress and rupture time data obtained to date. Data were initially obtained for given composite stresses and were related to volume percent fiber and rupture time. From such plots, the stresses for rupture in 1-, 10-, 100-, and 1000-hours were obtained as a function of fiber content. Tests were run in purified helium. The upper data points for 100 percent fibers were obtained from Lewis Research Center stress-rupture tests (ref. 15). It was very encouraging to note that the law-of-mixtures relationship applied over the entire portion of the curves (up to volume percentages of about 70 to 75 percent). As a first approach, the curves indicate that for a wide composition range, law-of-mixtures types of plots may be utilized to predict the strengths of composite materials in stress-rupture.

#### DEVELOPMENT OF FIBER-REINFORCED ENGINEERING MATERIALS

The material presented previously in this paper has been concerned with approaches of a relatively fundamental nature. Model systems have been discussed, and strengthening mechanisms were presented. In most of the work that has been done, materials combinations were selected to avoid or minimize reaction between fiber and matrix materials.

With the best technical knowledge that is available relative to materials considered for composites, it is possible to consider producing a composite material that will have useful properties. Some of the numerous attempts made to produce fiber-reinforced composites utilizing a developmental

approach will be presented in the next several figures. In addition, examples of some of the problems that might be encountered in combining materials for engineering composites will be illustrated.

Some typical problems that may be encountered are illustrated in the next two figures. Figure 31 shows a microstructure of some tungsten fibers embedded in a columbium-nickel matrix. The reaction that occurred at the periphery of the fiber apparently had not damaged the fiber by recrystallization phenomena (ref. 8). In this case, there appears, however, to have been stress cracking in the matrix and a penetration of these cracks into the fibers. In fact, the stresses were so great that in one case (in the right hand photograph) the fiber itself has been completely severed. Figure 32 shows a cross-sectional microstructure of some tungsten fibers embedded in a cobalt-alloy matrix (S-816)(ref. 8). In this case, the liquid matrix that was used in an attempt to infiltrate the fibers, plus the high temperature has partially dissolved the fiber and completely recrystallized that portion of the fiber not dissolved. Furthermore, the matrix became highly alloyed with the constituents of the fiber. To minimize such reactivity between the fiber and the matrix, various corrective steps might be taken. For example, where a fairly long time (1 hour) was used for the infiltration and consolidation process noted above; the time could be reduced. Another step might be to electroplate or form a diffusion barrier of some sort about the periphery of the fiber prior to infiltration. Still another method of avoiding the reaction is illustrated by figure 33. In this case, tungsten fibers are embedded in powdered nickel and the consolidation process was accomplished by solid-state sintering the composite. It should be recalled that small percentages of nickel in a liquid infiltrant had previously done considerable damage to the periphery of tungsten fibers. It is interesting to note that the solid-state sintering of tungsten fibers in a pure nickel matrix caused very little reaction to occur at the periphery of the fiber at the same temperatures that were used for the liquid infiltration studies. In fact, no recrystallization of the fiber was noted.

Solid-state sintering has also been utilized successfully by other investigators. Cratchley and Baker (see fig. 34), for example, dipped  $\text{SiO}_2$  fibers in aluminum and produced a coating of aluminum about the fiber (ref. 16). They then packed these in a hot press die and consolidated the composite using pressure and temperature. The composites so produced had ultimate tensile strengths at room and elevated temperatures that were very high. A product such as this has many engineering potentials; for example, in gas turbine engines. Stress carrying capacities of these composites were approximately 120,000 pounds per square inch, and high strengths were maintained to over  $300^\circ \text{C}$ . Cratchley, in some earlier work (ref. 9) which was described previously (see p.11), had embedded stainless-steel fibers in an aluminum matrix by a similar hot pressing process. Such materials, too, also could be utilized as engineering materials (see fig. 20).

In some work done by Jech, Weber, and Schwoppe (ref. 17), powder

metallurgy processes were combined with mechanical working processes to produce molybdenum reinforced titanium alloy composites. Figure 35 is a sketch of the working methods that were utilized to produce these composites.

Fibers that were 0.1 to 0.25 inch long were blended or ball milled with either pure titanium powder or a titanium alloy powder (Ti-6Al-4V). The randomly oriented molybdenum fibers so blended were then vacuum sintered along with the titanium or alloy matrix and extruded. The extrusion partially oriented the fibers as shown. The materials were then hot rolled. The rolling process oriented the fibers considerably; in fact, the fibers were elongated to as much as 6 inches in the final composite and reduced from 10 to 2 mils in diameter. Tensile strength, as a function of temperature and volume percent fiber, are given in figure 36 for molybdenum-reinforced titanium alloy matrix composites. At all temperatures indicated, the high temperature tensile strength is considerably above that of the strength of the alloy.

Some stress-rupture strengths for the molybdenum-reinforced titanium materials were also presented by Jech, Weber, and Swope in reference 17. These results are shown in figure 37. There the bar graphs represent rupture lives obtained at 800° and 1000° F at a stress level of 20,000 pounds per square inch. With only 10 volume percent fibers the life was increased by a factor of 10 at the lower temperature and by a factor of 1000 at the higher temperature.

Recently Baskey presented results obtained from numerous experiments on fiber-reinforced super alloys or high temperature alloy materials (ref. 18). Some of the matrix materials to which tungsten fibers were added as reinforcements were powders of cobalt, L-605, Ni-Cr, and stainless steel. Products were hot pressed in some cases, cold pressed and sintered in others, and some materials were worked subsequent to their initial fabrication. Room temperature and 2000° F tensile tests were made of these materials. Figure 38 represents some of the results obtained from hot pressed materials. When 10-mil-diameter tungsten fibers were added to a Nichrome matrix, the strengths at room temperatures of the composites were decreased relative to the Nichrome. A similar situation was true for a matrix of L-605. When a pure cobalt matrix was used and a small amount of fibers were added, the properties were lowered (this was true for both continuous and for random fibers). With larger volume percents of fibers, however, the strengths were increased considerably. When a composite containing 33 volume percent was further rolled or mechanically worked, the strength was further increased by an appreciable amount. It should be pointed out that these studies were exploratory or preliminary in nature and that fabrication problems arose in some cases that prevented the attainment of expected room temperature strengths.

However, elevated temperature tests at 2000° F of the same types of materials showed that the composites were much stronger than the matrix material (fig. 39). This was true even though only a small volume fraction

of fibers was used. This represents the second case where elevated temperature test results for fiber-reinforced materials were relatively better than low temperature test values. The first case described was that of Petrasek (ref. 10), which also involved tungsten fibers, but a different matrix (see figs. 24(a) and (b)). In cases where the test temperatures are greater than ductile-to-brittle transition temperature of the fibers, it might be expected that one of the main problems associated with the use of tungsten, namely, its brittleness at room temperature, would have been eliminated.

A novel method, that has been under investigation to produce composites of an engineering nature, is the method of directional solidification of castings. Recently, Ford, Hertzberg, and Lemke (ref. 19) have published results that show some idealized microstructures produced by casting an aluminum alloy with a fibrous aluminum-nickel intermetallic compound ( $\text{Al}_3\text{Ni}$ ) in the matrix. Figure 40 shows a cross section and longitudinal section of such a microstructure. Usually the problem associated with controlling a microstructure is that ingotism (solidification associated with mold or casting conditions) prevents the arrangement of the phases in idealized manner. Also, fiber-like growths, such as those shown in this figure, will usually not occur without special solidification techniques. The authors have grown both rods and parallel or lamellar plate-like structures in different alloys.

The above-mentioned investigators (ref. 19) also have grown fibers of chromium in a chromium-copper eutectic alloy. These fibers have whisker strengths. Figure 41 shows a stress-strain curve for a "whisker", which was obtained by digesting the copper-rich matrix from such a eutectic. The tensile strength of the whisker exceeded a million pounds per square inch. It is too early to speculate how far such casting approaches may be varied, but from an academic standpoint, as well as a potentially practical one, the work is most interesting. Finally some recent work done at the Lewis Research Center in which ceramic and refractory compound fibers were made by extrusion will be discussed briefly (refs. 20 and 21). While the composites to be described are not sufficiently developed to be considered useful as engineering materials today, indications have been obtained that this method shows considerable promise.

In the first of two studies, tungsten was used as a matrix, and refractory oxide or refractory compound fibers were formed by an "in situ" fabrication process. Composites were made by blending tungsten powders with the powdered oxides or compounds shown in table I. Initial compositions of constituents and nominal particle sizes are also given in the table along with melting points and densities of constituents. Blended powders were cold pressed and sintered into billets. Billets were extruded at a temperature of  $4200^\circ\text{F}$  at reduction ratios ranging from 8:1 to 20:1. Most of the specimens were extruded at a ratio of 8:1. This work was done to observe whether it was possible to elongate the compounds during the extrusion process or whether the compounds reacted with the tungsten, or both. It was suggested in reference 20 that "in situ" extrusion of a figure or a ceramic in a matrix has several inherent advantages. For one thing, there is a possibility that fibers so produced may be given strengths that



have never been given to the material by conventional methods of sintering or fabrication. The bond between the fiber and the matrix would be expected to be excellent, and perhaps the flow patterns within the fibers would be completely different from what they would be in a die or under other fabrication circumstances. In addition, fibers made by these methods would not be touched or damaged by handling, nor would they be affected by atmospheres other than the metal in which they are extruded.

Some of the composites that formed fibers or elongated ceramics are shown in figure 42. The microstructure of unreinforced tungsten is shown as a basis for comparison (fig. 42(a)) and a typical cross section that could be representative of all the fibered products shown in figure 42(b). Figures 42(c) to (f) are all oxides that have been fibered at the extrusion temperature. The length-to-diameter ratios for some of the oxides in the composites are indicated in figure 43 and were measured from photomicrographs and show that significant elongation of the oxides and the nitride materials was obtained. Some stress-rupture properties of these materials are shown in figure 43 for a temperature of 3000° F. The stresses to give 100-hour rupture lives for the different materials are shown. The strength increments due to the addition of the fibered zirconia, yttria, and the hafnia were slight since the strength of the final products was only slightly greater than the strength of the tungsten. In the case of the specimen with hafnium nitride, however, the property increase was substantial. At least two effects may have contributed to the strengthening of this composite other than fiberling; one, a dispersion effect and the other an alloying effect. Ways to determine which of the effects noted are predominant are under study. For a first approach, however, it was felt that the success obtained in actually elongating these materials was significant enough to warrant further studies and was exciting in itself. It is interesting also that the extrusion process used, including the proper selection of billet "can" (container) design permitted an elongation of such materials as a carbide and a boride. Some of the same oxides, as well as different oxides were then added to softer, more ductile matrix materials and extruded (ref. 21). Figure 44 represents the strength of some of these composites. These results are of a preliminary nature, but nevertheless, materials with a columbium matrix containing zirconium oxide fibered products are considerably stronger than columbium. The products have not reached the strengths obtained by the alloy F-48, a typical high strength alloy of columbium, but again as a first approach it is felt that the property increases have been significant. Additional work is underway and more will be presented in the future.

It should be obvious that the materials that have just been discussed are not in a form which can be used as engineering materials today. Strides that have been made are very significant, but considerable work must be done to permit such materials to be fabricated into actual components. The interest and effort in these areas are so great that it is almost axiomatic that workable, usable materials will result in the near future.

## POTENTIAL OF FIBER-METAL COMPOSITES

So much has been said about the potential of fiber-reinforced composites that it would seem almost redundant to discuss the matter further. Yet, the fundamental work that has been done along with the development efforts described in this paper have generated several concepts which might be worth considering. There is no question that the ultimate potential of fiber-reinforced composites will depend in large measure upon the ultimate strength or other properties of fibers that might be produced. Here, however, there are many "unknowns". It is not known, for example, what actual strengths might be produced in such fibrous materials as conventional metals, particularly, alloys, or in ceramics, hard metals or even semimetals, such as boron and carbon. Whiskers, of course, are expected to have strengths that are close to the theoretical strength of the materials and possibly will be the ultimate strength that will be achievable in a given type of material. More will be said about the whisker potential by other authors. Possibly, polycrystalline fibers of different types will be made that will have strengths approaching whisker strengths.

Actually, several types of fiber materials have been produced to date that exhibit unusual strength. Figure 45 shows some room temperature tensile properties of several types of polycrystalline fibers. Conventional, metallic alloy fibers are indicated at the left portion of the figure. It is interesting that one of the strongest metallic fibers that has been made is a steel wire that has a strength of about 600,000 psi (ref. 22). Numerous superalloy fibers have also been made, and some of these are considerably stronger as wires than they are in bulk form. This is true also at elevated temperatures. The strengths of some superalloy fibers are of the order of 300,000 psi (ref. 23). Refractory metal fibers such as tungsten, molybdenum alloys, columbium and tantalum, also have been shown to have high strength. One of the strongest wires that has been produced is tungsten, which has also achieved a strength of 600,000 psi. (ref. 24). At the right are indicated some of the strengths of materials other than conventional metals and alloys. These materials may be classified as ceramics, hard metals, and/or semimetals. In the case of materials like  $\text{SiO}_2$  and glass, for example, strengths of as much as 800,000 psi have been achieved (ref. 25). In the case of fibers such as aluminum oxide and boron, strengths of half a million psi have been obtained (refs. 26 and 27, respectively). In the case of graphite, strengths of as much as 400,000 psi have been achieved (ref. 28).

Under room or low temperature test conditions, many different types of fiber products might have strengths that are similar in magnitude and very high. At elevated temperatures, however, depending on the stability of the different materials, the strengths would be widely differing. In all cases the materials, however, will lose properties as the temperature of test is increased. In some cases a thermal treatment alone causes a degradation of the properties in the materials.

The conventional metallic materials indicated in figure 45 owe their properties, in part, to working and, in part, to microconstituents within the materials. A good portion of the strength of the materials then depends on the strain energy retained in the material and the stability of the microstructures. Relative to the conventional metals it may be generalized that alloys or materials containing precipitates or dispersoids would be expected to lose strength less rapidly with increasing temperature than relatively pure or simple metallic materials. The materials, such as the ceramics, hard metals, and semimetals, may gain their strength from other factors than stored energy. No attempt will be made to explain the high strength of these materials at room and elevated temperatures. Ceramics, although they often retain strength at high temperatures, also degrade in properties with increase in temperature. Materials such as the semimetals, carbon and boron, would tend to react with many metallic matrix materials at high temperatures. Ways to circumvent some of the instability problems will be discussed subsequently.

It should be recognized that many metallic fibers that have been made to date have been made for other purposes than reinforcement of metals. It is believed that it will be necessary to develop new fiber alloys that subsequently will be usable in composites. Similarly, matrix materials must be alloyed or made of materials that will permit the fiber to remain stable within it. Some fibrous materials must have a capacity for being strengthened in-situ in the matrix. Certainly much development work must be done to fully capitalize on the potential strength of metallic fibers. Ceramic, hard metal, and semimetals also will require a great deal of work to develop fibers specifically for reinforcement purposes. Some of these products might be developed by novel means, and it is entirely possible that, by reorienting the crystallites of such materials, or orientating the constituents within the materials, completely different products might be produced from those available today. Alloying such materials, as ceramics, too, is another method for producing a new generation of materials.

Since many of the potentially useful new combinations of fibers and matrix materials may react, it will be necessary to anticipate reactions. In some cases these reactions might be tolerable; in others they might have to be avoided. In many cases it would be ideal if complete heterogeneity could be maintained between the matrix and the fiber. It is conceivable, although not demonstrated as yet, that increases in properties might result from synergistic effects between the fibers and the matrix and permit the production of a composite material with properties far in excess of those that might be predictable from the strength of the individual materials. Materials such as ceramic (oxide) fibers, which have unusually high negative free energies of formation, would be expected to be more stable in a given matrix than would materials with lower negative free energy values. Thus stability considerations would be somewhat analagous to those for dispersion strengthened materials. Hard metals or semimetal fibers because of their reactivity with many matrices, could conceivably be used in relatively low melting materials where the exposure temperatures would never become great. Or, they might require a diffusion barrier or protective layer

that would prevent a reaction between the matrix fibers in higher use temperature materials. Diffusion barriers between fibers and matrices are going to prove necessary for many fiber-metal systems.

The next figure (fig. 46) might be associated with the stability of the relative materials comprising a composite. It illustrates, schematically, concepts relative to using a high melting point fiber in a low melting point matrix. The illustration is based on actual data that exist today, for both model and developmental fiber-metal systems. Cases in point may be observed in reference 10 that involve the embedding of tungsten fibers and copper, and testing them at elevated temperatures; ref. 29, which involves the embedding of aluminum oxide or sapphire whiskers in a silver matrix; and the incorporation of glass fibers in aluminum or in aluminum alloys (refs. 30 and 31). The illustration here is one based on a semilogarithmic plot of the tensile strengths of a full-length fiber-reinforced composite versus homologous temperatures of the matrix. At the top of this figure, homologous temperatures of a typical fiber are presented. It is evident that at the melting point of the matrix, which is of course at a homologous temperature of 1.0, the fiber in this composite would be at a homologous temperature of only 0.35. The resulting composite then would have strengths maintainable to very high percentages of the melting point of the matrix. To accomplish this type of strengthening for high temperature materials, there must be some degree of heterogeneity between the fiber and matrix material. The level of the strength of the composite, relative to that of the matrix, would of course depend on the strength of the fibers selected and the volume percent of the fibers utilized and could be relatively more or less than illustrated. Where discontinuous fibers are used, it should be assumed that fiber lengths would be great enough so that bond or matrix shear strengths at the fiber-matrix interface would not be exceeded. For composites to be used at low temperatures, the melting point differential between the fiber and the matrix may not be as important as for high use temperature composites. Such composites might be designed using strength and density considerations rather than melting point or thermal stability relationships. Possibly too, fibrous materials might be incorporated in metallic matrices having melting points nearly equal to those of the fibrous materials. Such composites could then be used at temperatures closer to the melting point of the fibers. Possible examples might be: aluminum alloys in aluminum, copper alloys in copper, alloy steels in iron and more corrosion resistant weaker steels, superalloys in steels and more corrosion resistant alloys, tungsten in tantalum, ceramics in refractory metals, and so forth.

Because time, temperature and stresses are interrelated parameters associated with the high temperature properties of materials, it is difficult to present a relatively concise, graphical, or pictorial representation of the potential of high temperature fiber-reinforced composites. Nevertheless, an attempt will be made to illustrate at least some of the elevated temperature potentials of composites, alloys, and dispersion strengthened materials. Figure 47 will help illustrate the elevated temperature potential of fiber-reinforced superalloys under tensile conditions compared with dispersion strengthened or normally

alloyed superalloy materials. It should be emphasized at the outset that the values presented will not do justice to some of the materials which are better relative to other materials for long time high temperature applications. It should also be emphasized that, even though the curves that are presented pertain to superalloy systems, similar sets of curves could also be drawn up for other matrix systems. For example, similar sets could be drawn up for aluminum, copper, or refractory metal base materials. If the plots of figure 47 and of such systems as those noted above were made using a homologous temperature scale, the stress carrying capacities at given homologous temperatures of many of the different materials would be of the same general magnitudes. Even fiber stress magnitudes would not be radically different from magnitudes of matrix strengths. The comparisons of figure 47 then, because they cover an actual use temperature range of great interest, more graphically illustrate the relative potentials of the different types of materials.

The curves representing the superalloys should be considered the basis for comparison. The lower of these curves represents strengths of alloys presently developed. Developments in this area are difficult to predict, and so an arbitrary 25 percent stress-increase was assumed to be possible for the different temperature levels. Even with no improvement in tensile properties, the strengths shown by the lower superalloy curve are high relative to the best-known dispersion strengthened nickel materials (e.g., TD-Ni represented by the lowest curve). Dispersion strengthened materials show up much stronger in similar plots of rupture-strengths versus test temperatures. A newer generation of dispersion strengthened materials expected in the relatively near future may have properties such as those given by the next highest curve. Except for the very high temperature conditions, these strengths do not exceed those of the conventionally produced alloys. The potential strengths of dispersion strengthened materials may be calculated by equating (on homologous temperature basis) the ratio of S.A.P. aluminum strength to pure aluminum strength to the ratio of the desired dispersion strengthened material strength to the matrix strength (e.g.,  $\text{S.A.P. strength/Al strength} = \text{Ni - dispersion strengthened material/Ni strength}$ ). These values, which may be questioned from several standpoints, were then further manipulated graphically to give values such as those shown in the upper curve (at low temperatures). Such analogue-tensile strengths are not expected for such high melting point materials as Ni, although values calculatable in similar manners may possibly be achieved for long time stress-rupture conditions. Certainly, Ni or superalloy dispersion strengthened materials will be produced considerably better than those available today. Even high temperature refractory fibers may be strengthened by dispersoids to yield better high temperature fibers than those available today. Consider then the two fiber curves, which were calculated from strengths of materials known today. The lower curve would have to be greater than the lower superalloy curve, because fibers stronger than the matrix would be used. The high temperature portion of the curve should have values considerably greater than those of the next generation of superalloys or dispersion strengthened materials. With increasing fiber development (i.e., fibers for incorporation into metals) such as might be

expected from refractory metal alloys, new polycrystalline ceramics, and coated reactive materials, the strengths represented by the upper fiber curves might be achieved. Such composites would have strengths of over 200,000 psi at 2000° F.

The long time high temperature (i.e., stress-rupture) possibilities for use of fibers may be illustrated with figure 48. Here, a hypothetical design condition has been selected. A composite with mechanical properties such as those desired; namely, 15000 psi, 1000 hours, and 2000° F would be most desirable for air breathing gas turbines, for example, if it could be made oxidation resistant. The best superalloy properties today are about 8000 psi; wrought products are even less strong. Commercial TD-Ni has a strength of 7000 psi. Other Ni or superalloy base materials are expected from several sources that will meet the 15000-psi goal. With known fiber and matrix materials available today, the high strengths shown on the right-hand portion of the figure are possible.

#### SUMMARY

The law-of-mixtures relationship has been shown to represent the behavior of some fiber-metal composites under room temperature and elevated temperature tensile conditions as well as under stress-rupture conditions. Creep resistant, high strength composites as well as low temperature fiber composites appear to have great promise. Some attempts have been made to produce practical engineering materials utilizing fundamental as well as developemental concepts. Encouraging results have been obtained in the production of these materials. These results coupled with the potentials indicated from more fundamental programs suggest that unusual fiber-metal composites will be produced in the near future. These mechanism studies should further encourage the development of practical engineering materials. Fibrous materials, specifically designed for incorporation in a metallic matrix must be developed before fiber-metal composites even begin to approach their achievable potentials.

## REFERENCES

1. Jech, R. W.; McDanels, D. L.; and Weeton, J. W.: Fiber Reinforced Metallic Composites, Composite Materials and Composite Structures. Proc. Sixth Sagamore Ordnance Materials Conf., Aug. 18-21, 1959, pp. 116-143.
2. McDanels, D. L.; Jech, R. W.; and Weeton, J. W.: Metals Reinforced with Fibers. Metal Prog., vol. 78, no. 6, Dec. 1960, pp. 118-121.
3. McDanels, David L.; Jech, Robert W.; and Weeton, John W.: Stress-Strain Behavior of Tungsten-Fiber-Reinforced Copper Composites. NASA Technical Note D-1881, Oct. 1963.
4. Dietz, A. G. H.: Design Theory of Reinforced Plastics. Fiberglass Reinforced Plastics, Reinhold Pub. Corp., 1954, pp. 175-180.
5. Kelly, A.; and Tyson, W. R.: Fibre Strengthened Materials. Proceedings of the 2nd International Materials Symposium (California, 1964) New York and London (John Wiley) also Dept. Metallurgy, Univ. of Cambridge, England.
6. Jech, R. W.: Unpublished data.
7. Piehler, Henry R.: Plastic Deformation and Failure of Silver-Steel Filamentary Composite Materials. Mass. Inst. Tech. Aeroelastic/Structures Res. Lab. TR-94-5, Nov. 1963. Also Trans. Met. Society. AIME, vol. 233, no. 1, Jan. 1965, pp. 12-16.
8. Petrasek, Donald W.; and Weeton, John W.: Alloying Effects on Tungsten-Fiber-Reinforced Copper-Alloy or High-Temperature-Alloy Matrix Composites. NASA Technical Note D-1568, Oct. 1963.
9. Cratchley, D.: Factors Affecting the UTS of a Metal/Metal-Fibre Reinforced System. Powder Metallurgy, no. 11, 1963, pp. 59-72.
10. Petrasek, D. W.: Elevated Temperature Tensile Properties of Tungsten Fiber Reinforced Copper and Copper Alloy Composites. To be published.
11. Petrasek, D. W.; Signorelli, R. A.; and Weeton, J. W.: Elevated Temperature Tensile Properties of Discontinuous Tungsten Fiber Reinforced Copper Composites. Proposed NASA TN.
12. Stowell, E. Z.; and Liu, T. S.: On the Mechanical Behaviour of Fibre-Reinforced Crystalline Materials. J. of Mech. Phys. of Solids, vol. 9, 1961, pp. 242-260.

13. Kelly, A.; and Davies, G. J.: The Principles of the Fibre Reinforcement of Metals. Metallurgical Reviews, vol. 10, no. 37, 1965, pp. 1-79.
14. McDanel, D. L.; Signorelli, H. W.; and Weeton, J. W.: Stress-rupture Behavior of Tungsten Fiber Reinforced Copper Composites. Proposed NASA TN.
15. McDanel, D. L.; and Signorelli, R. A.: Stress-Rupture Properties of Tungsten Fibers (Wire) From 1200° to 2500° F. Proposed NASA TN.
16. Cratchley, D.; and Baker, A. A.: The Tensile Strength of a Silica Fibre Reinforced Aluminum Alloy. Metallurgia, vol. 69, no. 414, Apr. 1964, pp. 153-169.
17. Jech, R. W.; Weber, E. P.; and Schwoppe, A. D.: Fiber-Reinforced Titanium Alloys. Reactive Metals, vol. 2, ed. by W. R. Clough, 1959.
18. Baskey, R. H.: Fiber Reinforcement of Metallic and Nonmetallic Composites. Contract AF33(657-7139, ASD-TDR - 63-619, AD 417390), July 1963.
19. Ford, J. A.; Hertzberg, R. W.; and Lemkey, F. D.: Analytical and Experimental Investigations of the Fracture Mechanisms of Controlled Polyphase Alloys. United Aircraft Corp., Final Report, Nov. 29, 1963.
20. Quatintetz, Max; Weeton, John W.; and Herbell, Thomas P.: Studies of Tungsten Composites Containing Fibered or Reacted Additives. NASA TN D-2757, 1965.
21. Jech, R. W.; Weeton, J. W.; and Signorelli, R. A.: Ceramic Fiber Reinforced Refractory Metal Composites for High Temperature Use. Proposed NASA TN.
22. Roberts, D. A.: Physical and Mechanical Properties of Some High-Strength Fine Wires. Battelle Memorial Institute. DMIC Memo 80, Jan. 1961.
23. Private communication from C. A. Gorton and C. C. McMahon.
24. Agte, C.; and Vacek, J.: Tungsten and Polybdenum. NASA TT F-135, 1963.
25. Morley, J. G., et al.: Strength of Fused Silica. Phys. and Chem. Glasses. 5 (1) pp. 1-10, Feb. 1964.
26. Private communication from Babcock and Wilcox.
27. McCreight, L. R.; Rauch, H. W. L.; and Sutton, W. H.: A Survey of The Art of Ceramic and Graphite Fibers. AFML TR 65-105, May 1965.
28. Private communication from Union Carbide Corp.



29. Sutton, Willard H.: Investigation of Whisker-Reinforced Metallic Composites. General Electric Co. SSL 63-1, 1963.
30. Whitehurst, H. B.: Investigation of Glass-Metal Composites. Third Quarterly Report, Owens-Corning Fiberglass Corporation.
31. Whitehurst, H. B.; and Ailes, H. B.: Investigations of Glass-Metal Composites. Fifth Quarterly Report, Owens-Corning Fiberglass Corp., Contract Nord 15764, Sept. 1956.

TABLE I. - MATERIALS USED IN STUDY TO STRENGTHEN TUNGSTEN BY "IN SITU" FIBERING  
OR REACTION BETWEEN ADDITIVES AND MATRICES (ref. 20)

Material	Source	Nominal purity, weight percent	Nominal average Fisher particle size, $\mu$	Melting point, $^{\circ}\text{F}$	Density, g/ml
Tungsten + 5 vol- ume percent $\text{HfO}_2$	General Electric Co. Curtiss-Wright Corp.	99.96 99.74	1.2 2.0	6130 -----	19.30 -----
$\text{ZrO}_2$	Titanium Alloy Mfg. Co.	98.80	2.0	4892	5.49
$\text{Y}_2\text{O}_3$	General Electric Co.	-----	1.7	4370	4.84
$\text{HfO}_2$	Wah Chang Corp.	99.92	1.9	5090	9.68
$\text{ThO}_2$	Lindsey Light & Chem. Co.	-----	2.1	5522	10.03
$\text{HfB}_2$	The Carborundum Co.	93.3	6.8	5880	11.20
$\text{HfN}$	The Carborundum Co.	(2.9 Zr, Th+C) 96.6	4.6	5990	14.00
$\text{HfC}$	The Carborundum Co.	(3.0 Zr) 95.4	4.2	7030	12.70
$\text{TaC}$	The Carborundum Co.	(4.6 Zr, Th+B) 99.85	5.0	7020	14.65

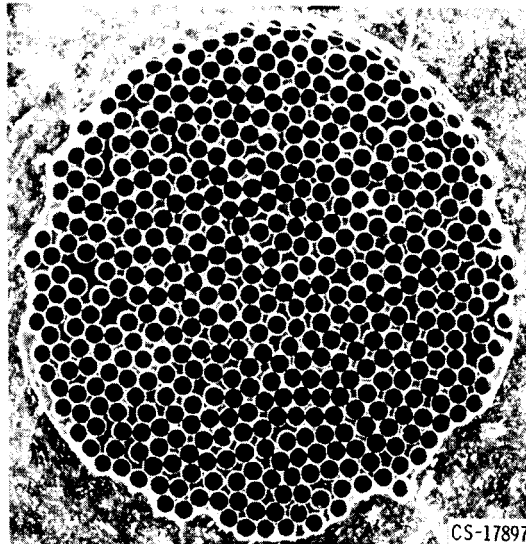


Figure 1. - Tungsten-reinforced copper composite containing 483 5-mil-diameter wires. Transverse section; unetched (ref. 3); X50.

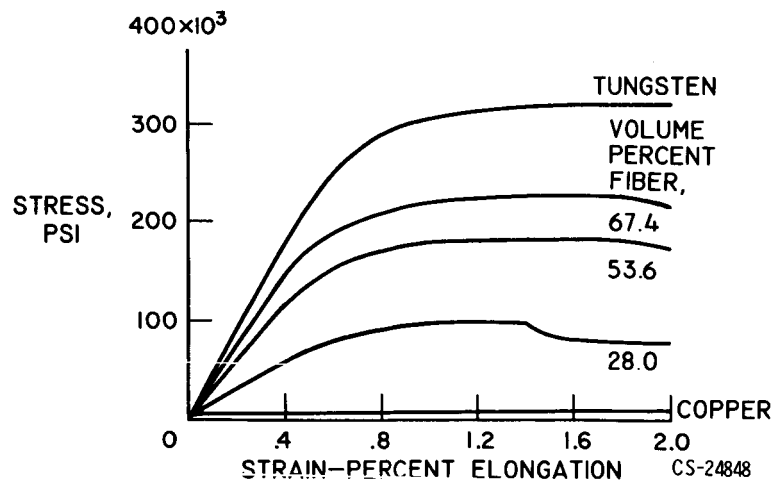


Figure 2. - Stress-strain curves for tungsten wire, copper, and composites reinforced with continuous 5-mil-diameter tungsten wire (ref. 3).

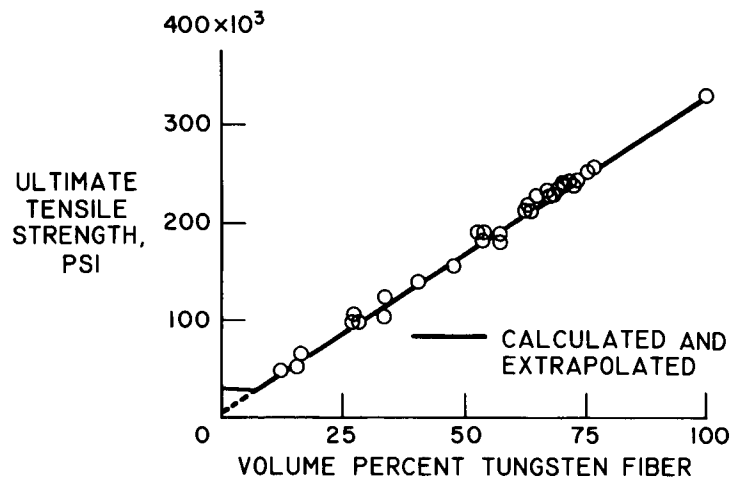


Figure 3. - Ultimate tensile strengths of tungsten-  
fiber-reinforced copper composites; continuous 5-mil-  
diameter tungsten fibers (ref. 3).

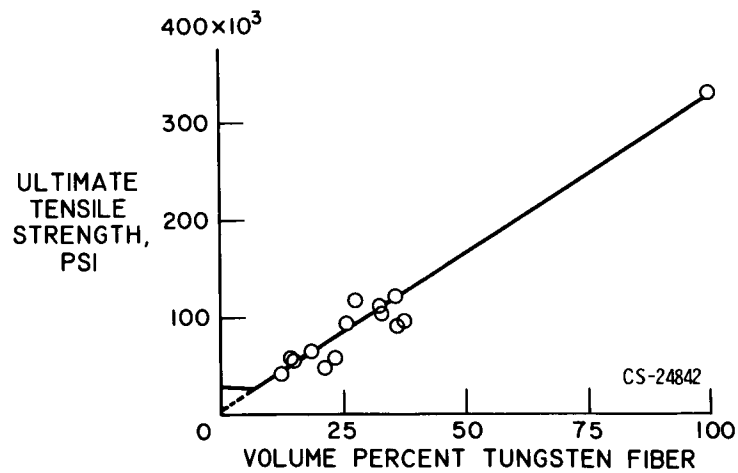


Figure 4. - Ultimate tensile strengths of tungsten-  
fiber-reinforced copper composites; discontinuous 5-  
mil-diameter tungsten fibers (ref. 3).

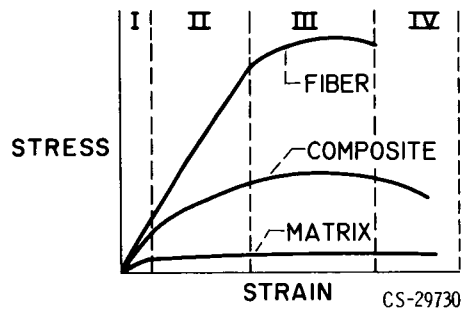


Figure 5. - Schematic illustration of four stages of deformation of fiber, matrix, and composite. Stage I: elastic deformation of both fiber and matrix; stage II: elastic deformation of fiber, plastic deformation of matrix; stage III: plastic deformation of both fiber and matrix; stage IV: failure of both fibers and matrix (successive failure of fibers) (ref. 3).

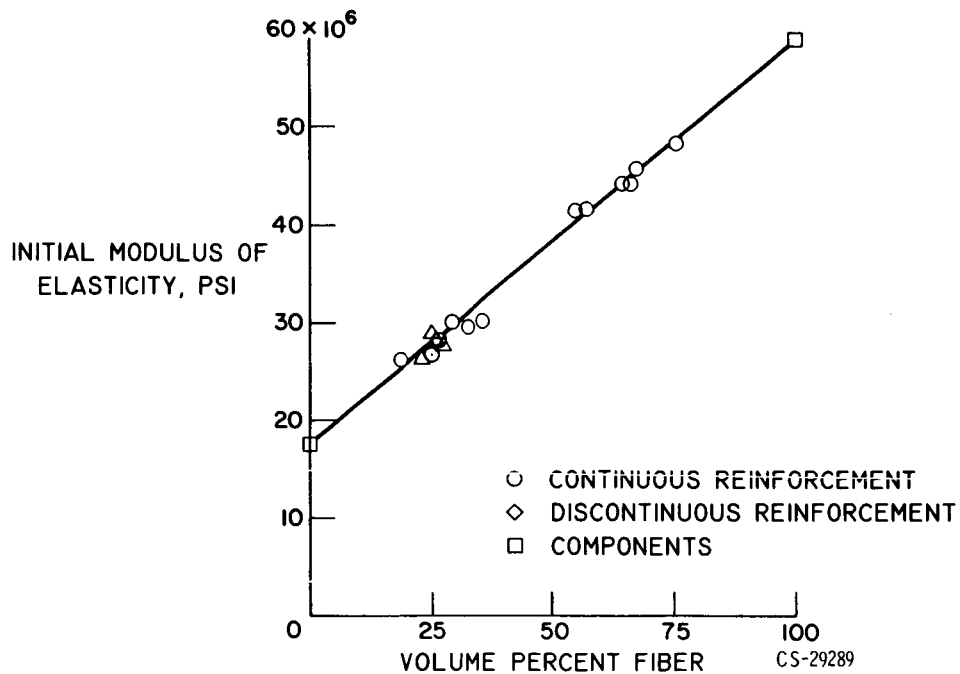


Figure 6. - Initial modulus of elasticity of tungsten, copper, and composites reinforced with continuous and discontinuous 5-mil-diameter tungsten fibers (ref. 3).

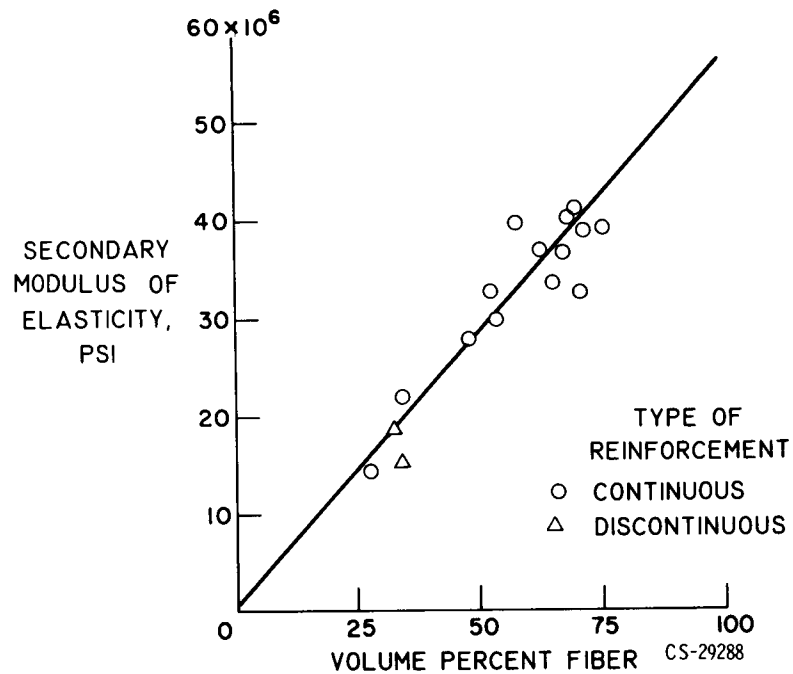


Figure 7. - Secondary modulus of elasticity of composites reinforced with continuous and discontinuous 5-mil-diameter tungsten fibers (ref. 3).

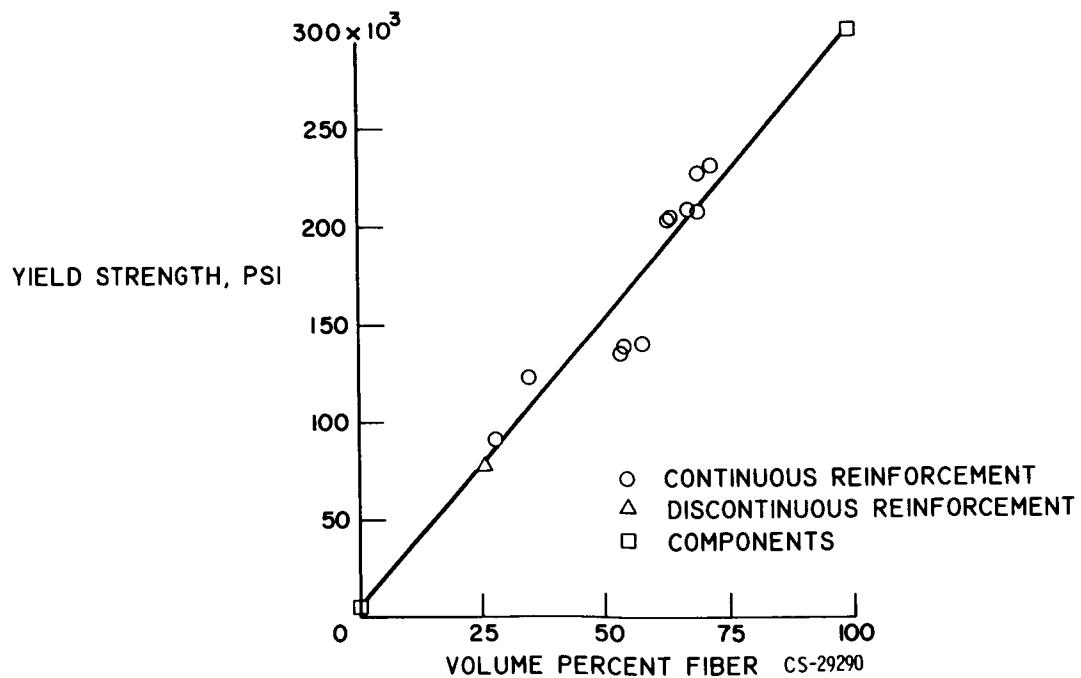


Figure 8. - Yield strength (based on secondary modulus) of composites reinforced with continuous and discontinuous 5-mil-diameter tungsten fibers (ref. 3).



Figure 9. - Longitudinal section through failed composite showing fracture edge and "neck-down" of fibers; 3-mil-diameter continuous tungsten fibers in copper matrix (ref. 3); X50.

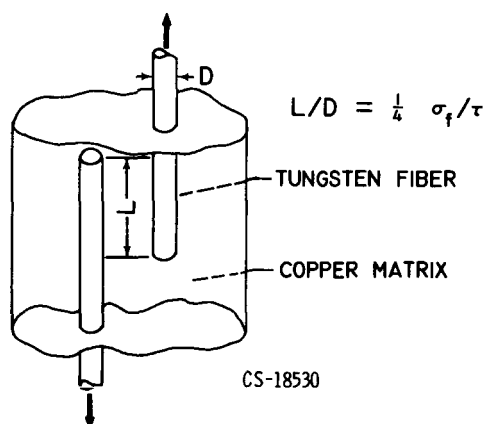


Figure 10. - Schematic illustration of shear load transfer mechanism in fiber-reinforced composites reinforced with discontinuous fibers (refs. 1 and 3). (Length L corresponds to value of L used in equation (2).)

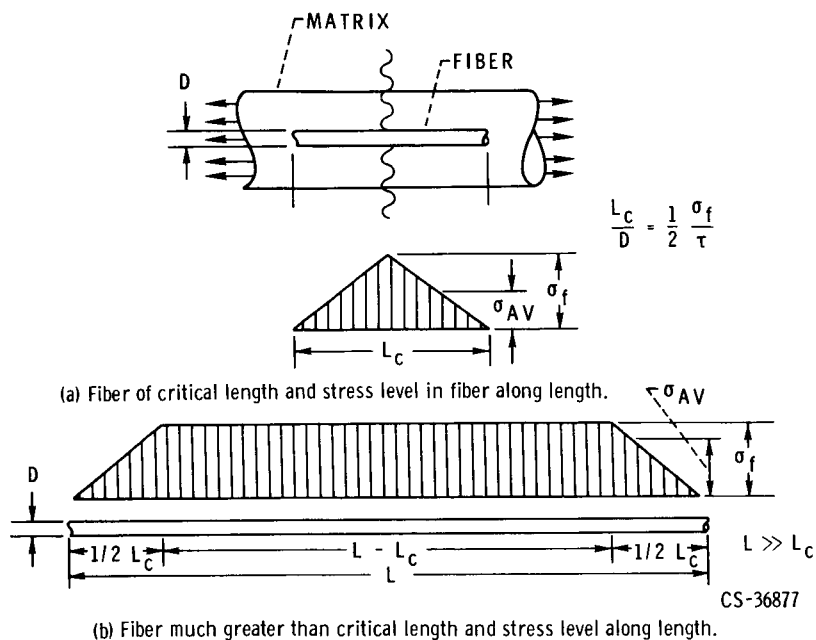


Figure 11. - Schematic illustration of stresses in critical length of fiber in matrix and effect of increasing length upon average fiber stress.

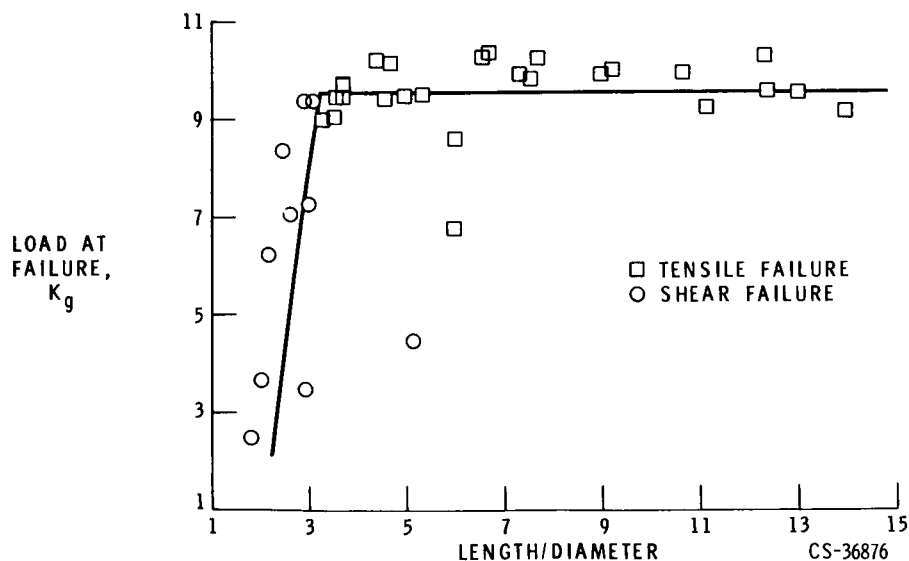


Figure 12. - Experimentally determined length-to-diameter ratios for tungsten fibers in copper (pull-out load method; room temperature). Interfiber distance, 1.6 mils (ref. 6).



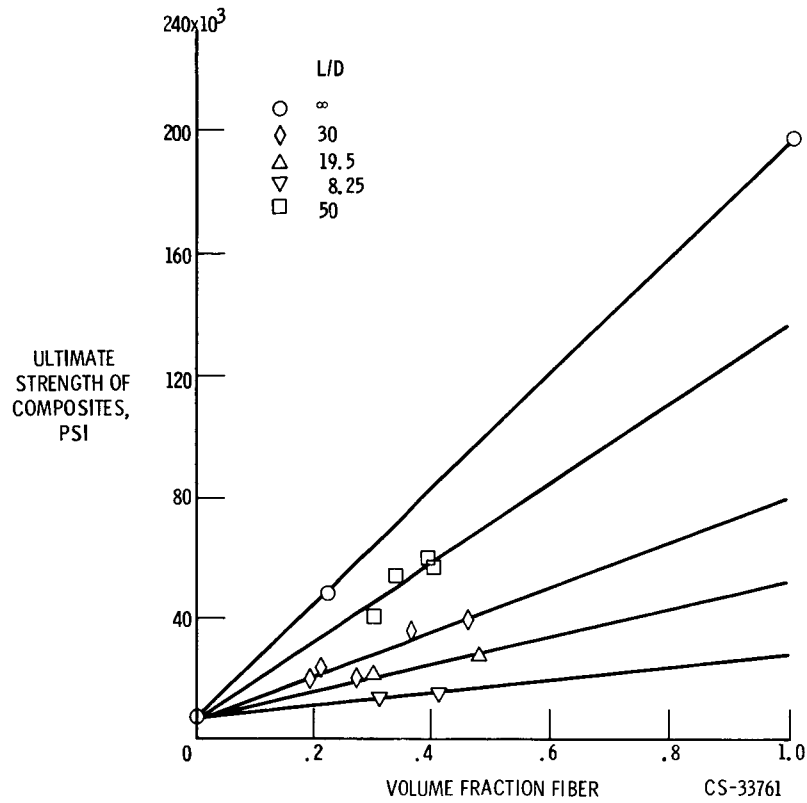


Figure 13. - Ultimate tensile strengths of tungsten-fiber - copper-matrix composites as a function of volume fraction of fibers and length-to-diameter ratios. Temperature, 600° C (1212° F); 0.008-inch-diameter fibers (ref. 5).

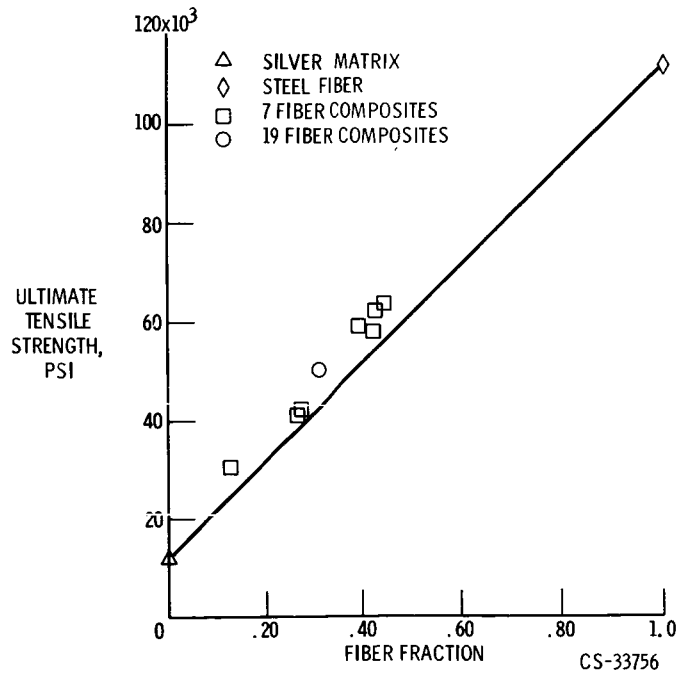


Figure 14. - Ultimate tensile strengths of steel-fiber-reinforced silver composites (ref. 7).

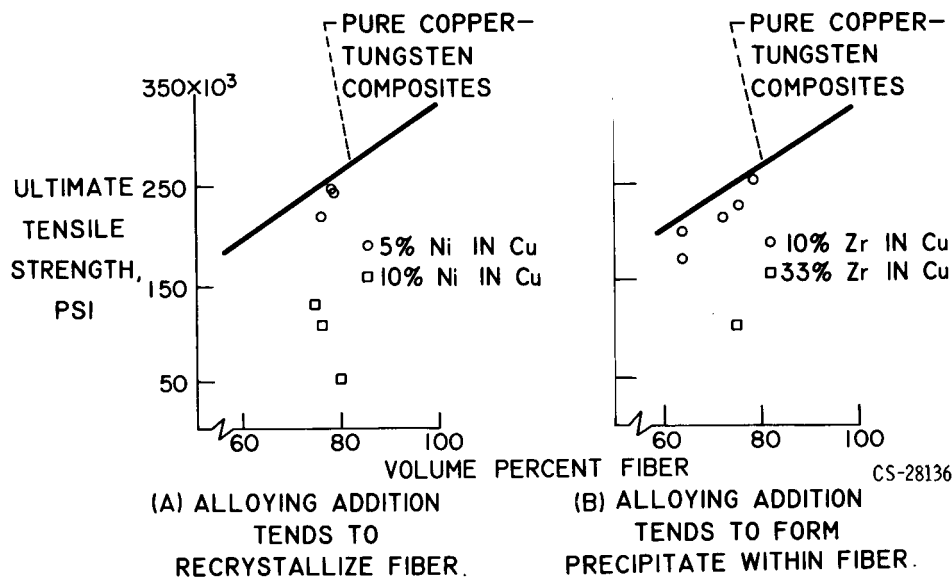


Figure 15. - Strength-composition diagrams comparing tungsten-fiber-reinforced copper composites to tungsten-fiber-reinforced copper alloy composites (ref. 8).

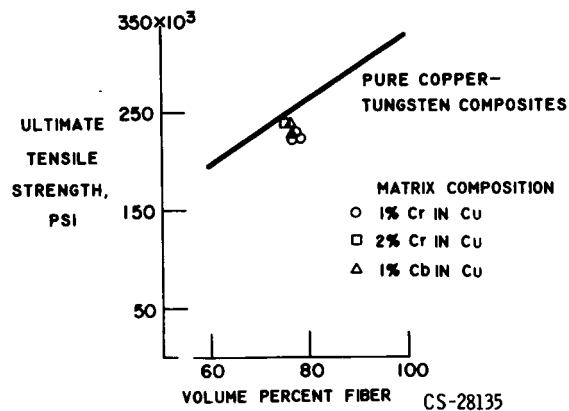
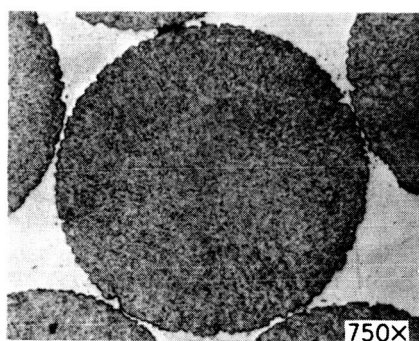
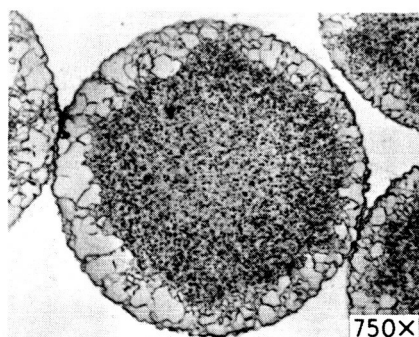


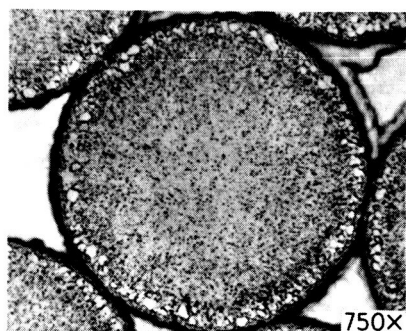
Figure 16. - Strength-composition diagrams comparing tungsten-fiber-reinforced copper composites to tungsten-fiber-reinforced copper alloy composites. Alloying additions mutually soluble with fiber material (ref. 8).



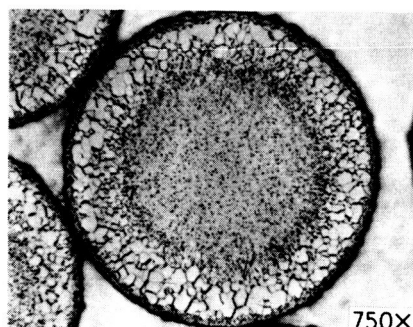
(A) Cu-5 PERCENT Ni MATRIX.



(B) Cu-10 PERCENT Ni MATRIX.



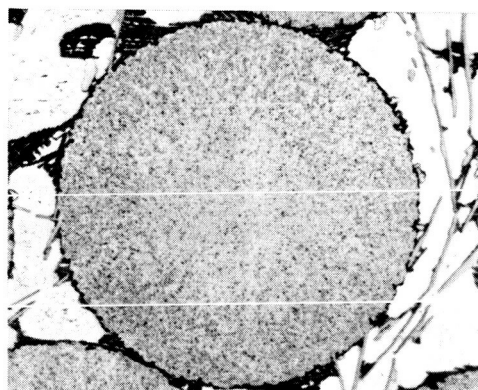
(C) Cu-1 PERCENT Co MATRIX.



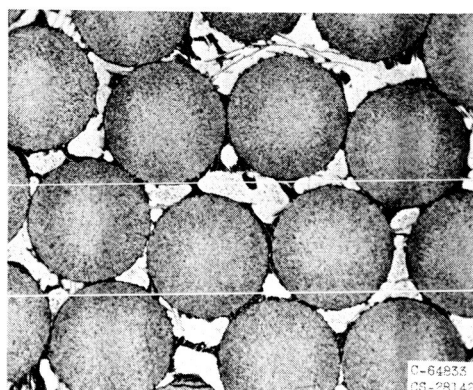
(D) Cu-5 PERCENT Co MATRIX.

CS-29265

Figure 17. - Tungsten fibers in copper alloy matrices; transverse sections, as infiltrated. Diffusion penetration, recrystallization reaction zones (ref. 8).



X750



X250

C-64833  
CS-28142

Figure 18. - Tungsten fibers in copper alloy matrix; transverse section, as infiltrated. Copper-10 percent zirconium matrix (ref. 8).

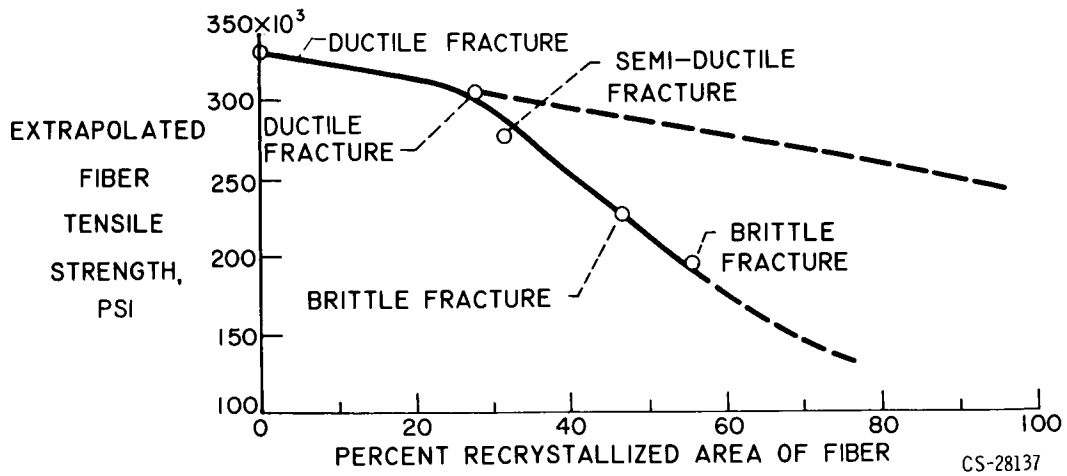


Figure 19. - Fiber tensile strength as a function of percent recrystallized area of fiber; matrix of copper plus 5 percent cobalt (ref. 8).

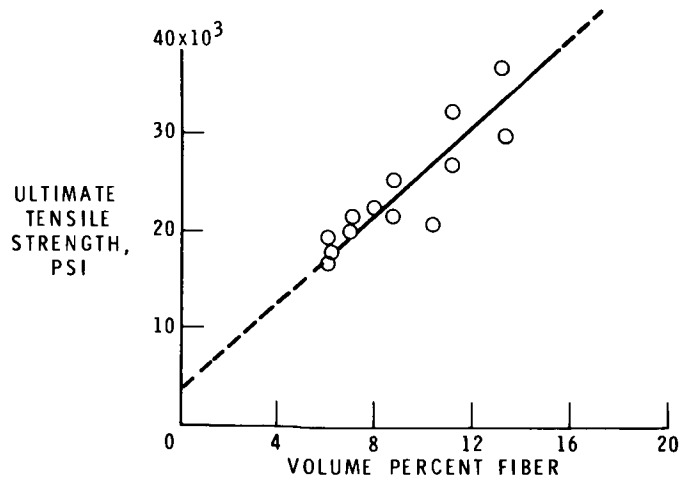


Figure 20. - Strength versus composition diagram for stainless-steel fibers in aluminum; 0.002-inch-diameter stainless-steel fiber in aluminum matrix (ref. 9).

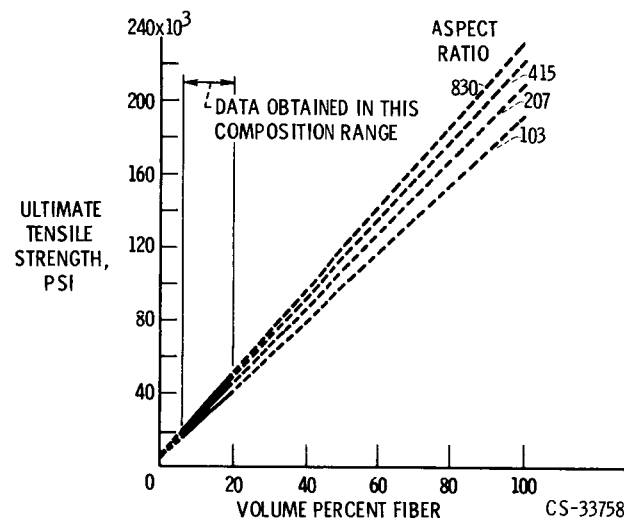


Figure 21. - Effect of aspect ratio upon strength-composition relationship for stainless-steel-fiber-reinforced aluminum composites; discontinuous 2-mil-diameter fibers (ref. 9).

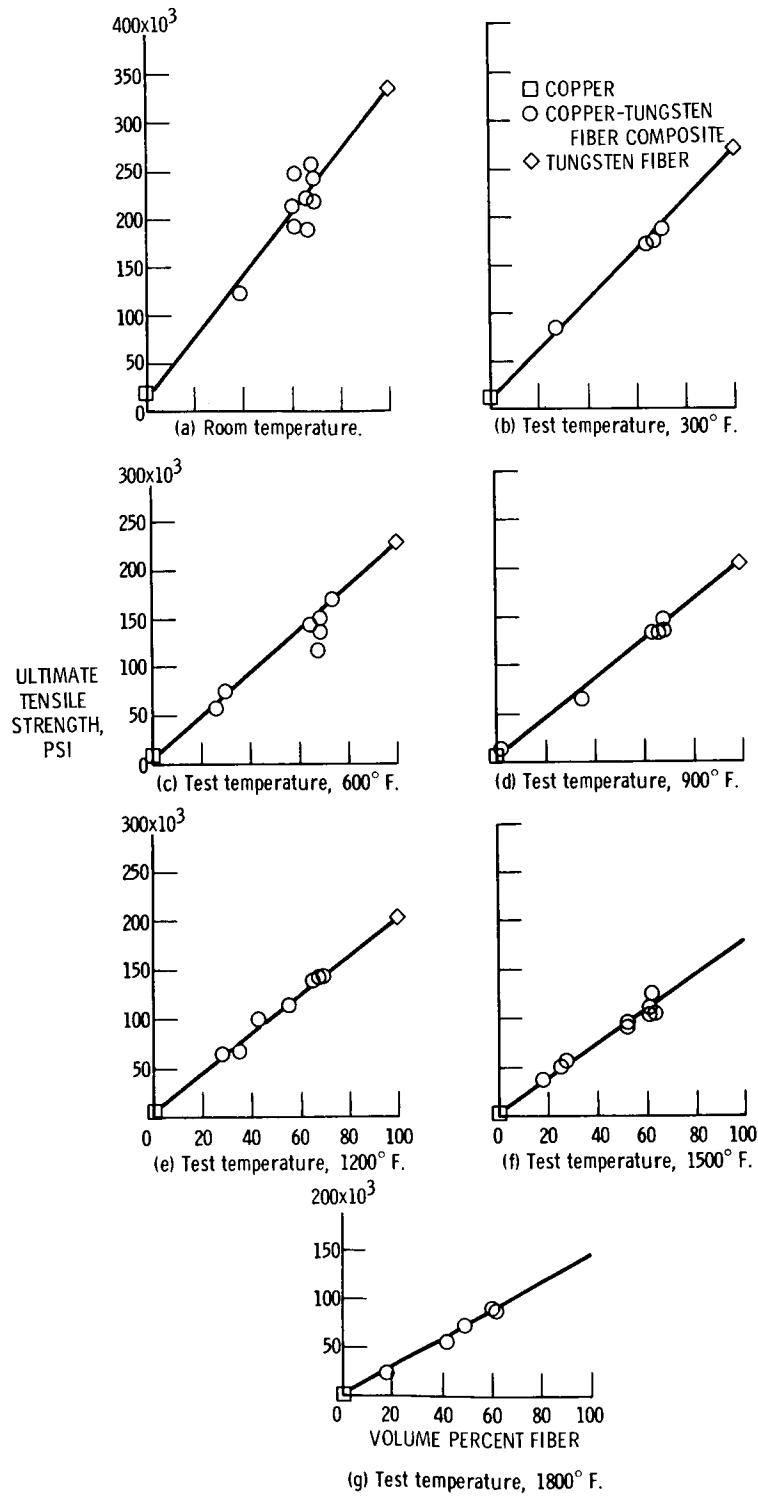


Figure 22. - Tensile strength-composition diagrams for tungsten-fiber-reinforced copper composites as a function of temperature; continuous tungsten fibers (ref. 10).

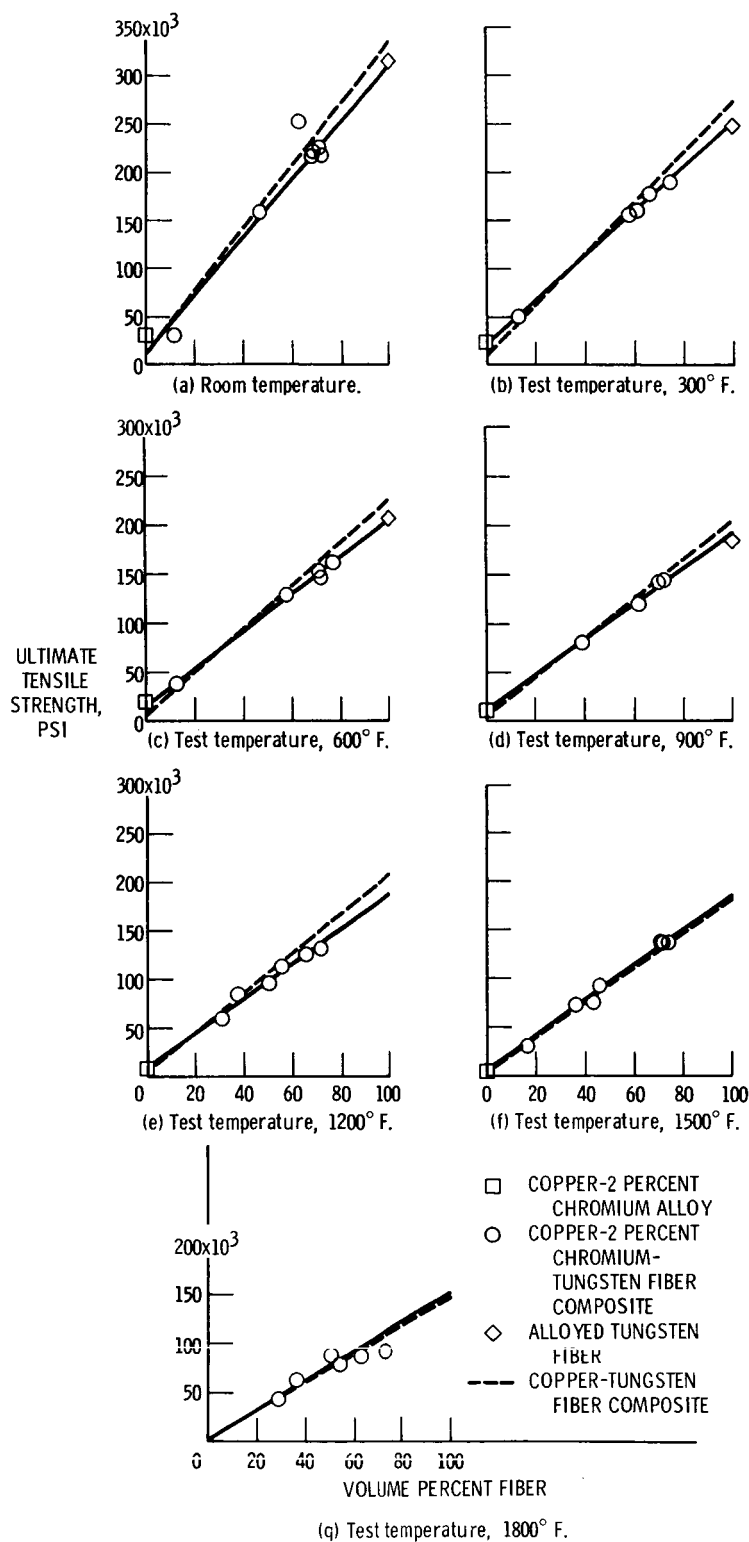


Figure 23. - Tensile strength-composition diagrams for tungsten-fiber-reinforced copper alloy composites as a function of temperature; continuous tungsten fibers in copper plus 2 percent chromium alloy.

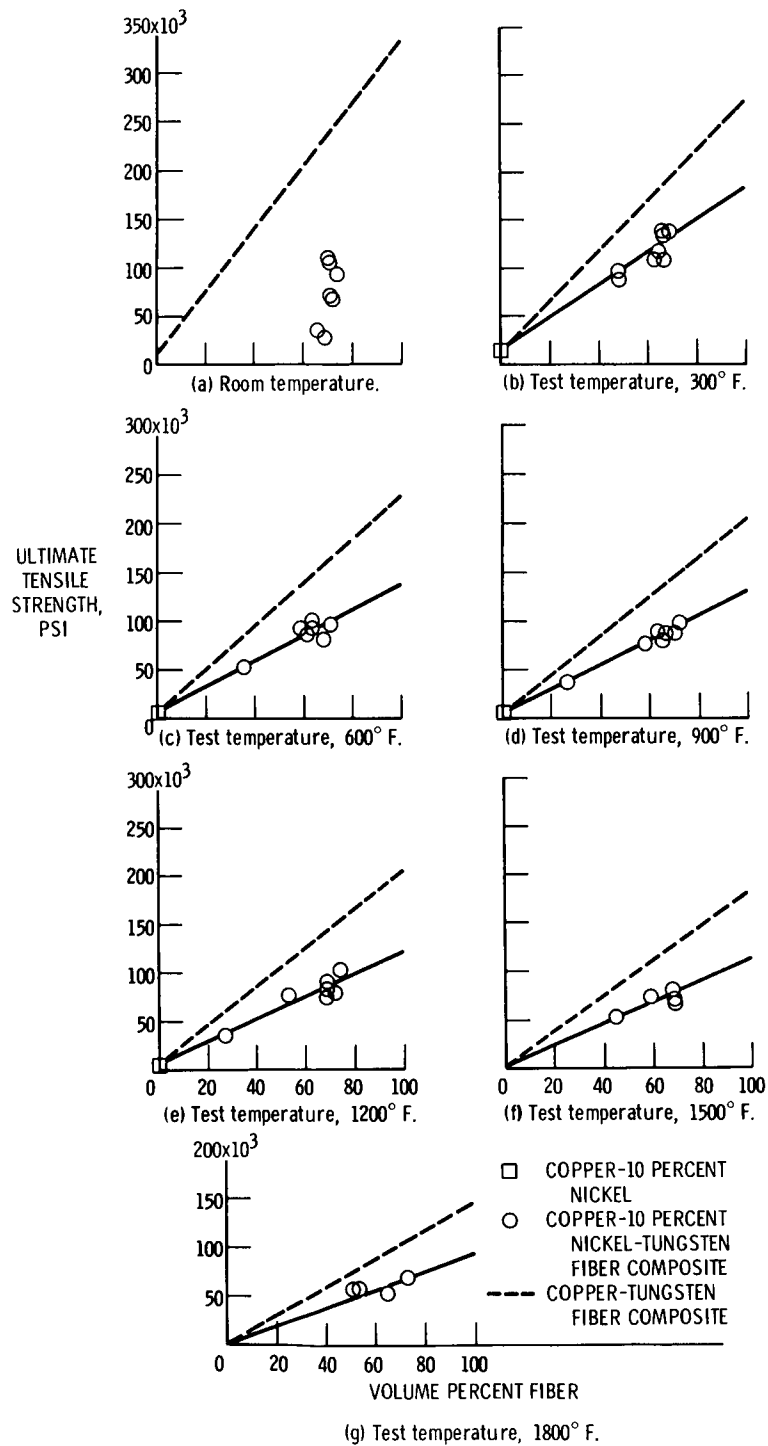


Figure 24. - Tensile strength-composition diagrams for tungsten-fiber-reinforced copper alloy composites as a function of temperature; continuous tungsten fibers in copper plus 10 percent nickel alloy matrices.



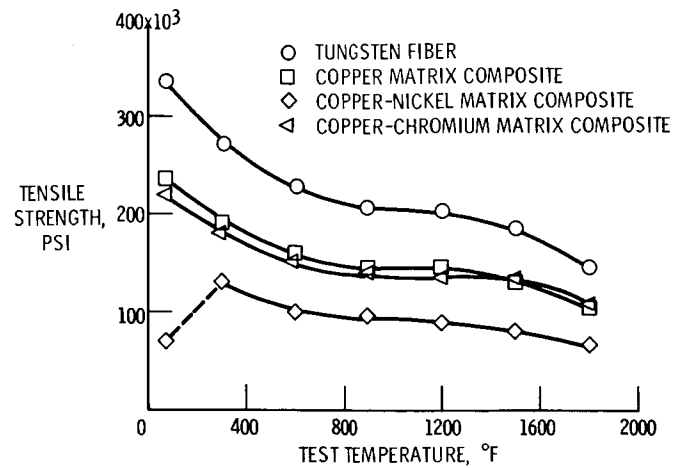


Figure 25. - Tensile strength as a function of test temperature for composites containing 70 volume percent fibers and for individual constituents; continuous tungsten fibers; matrix materials, copper - 2 percent chromium and copper - 10 percent nickel.

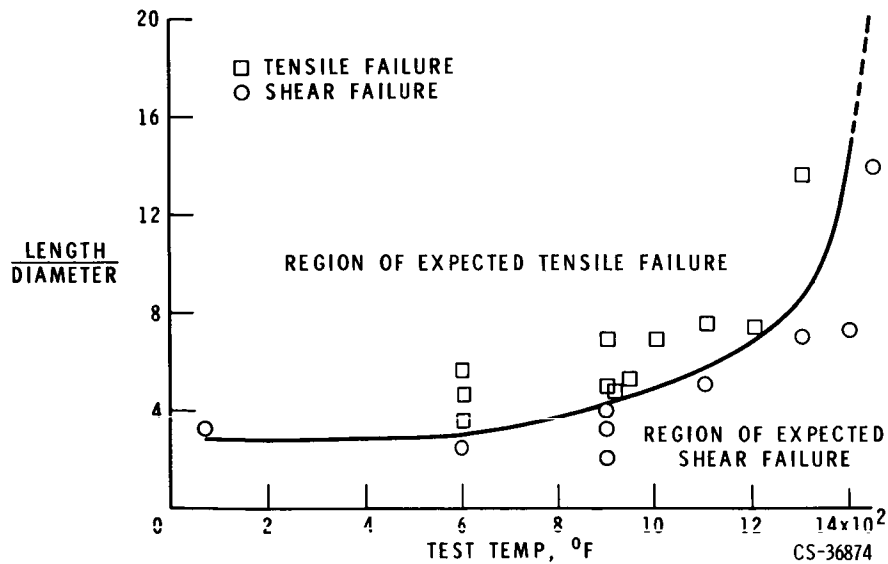


Figure 26. - Experimentally determined length-to-diameter ratios as a function of temperature for tungsten fibers in copper. Interfiber distance, 1.6 mils (ref. 6).

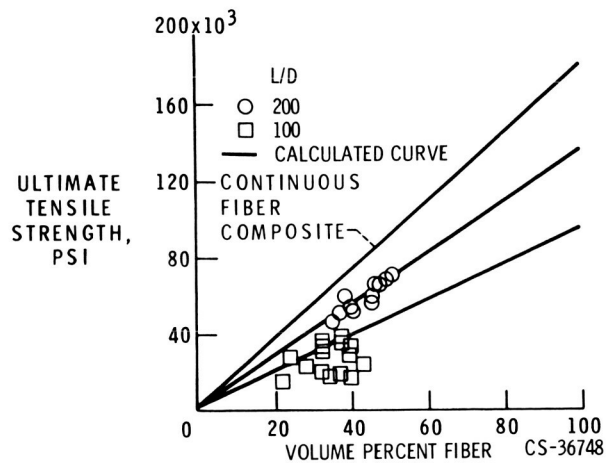
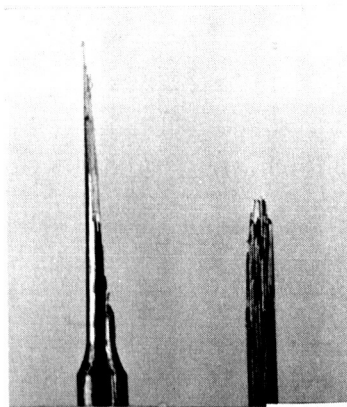


Figure 27. - Tensile strength at 1500° F as a function of volume percent fibers and fiber length for tungsten-fiber-reinforced copper composites (ref. 11).

$$\sigma_c = \frac{\tau}{\sin \phi \cos \phi}$$



CS-36761

Figure 28. - Typical examples of test specimens that failed in tension or shear (ref. 11).

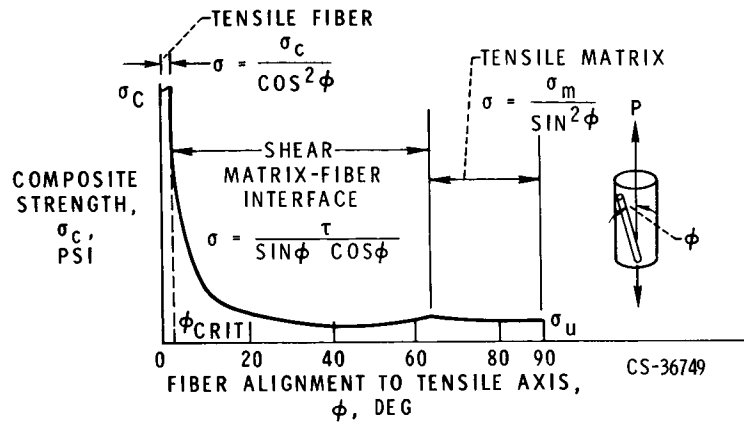


Figure 29. - Failure mode as a function of alignment of fibers in a discontinuous fiber-reinforced composite (ref. 11).

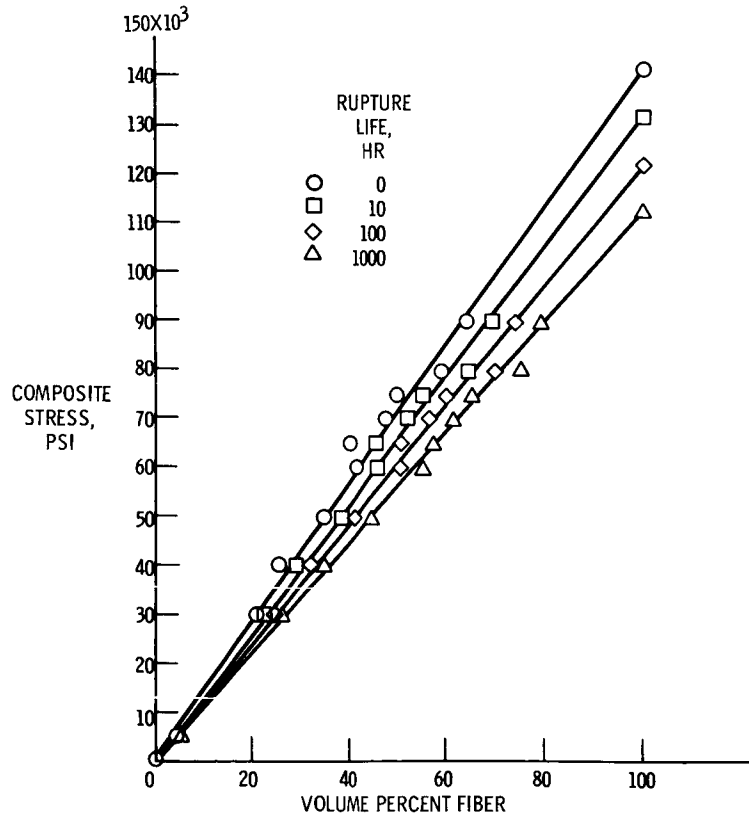
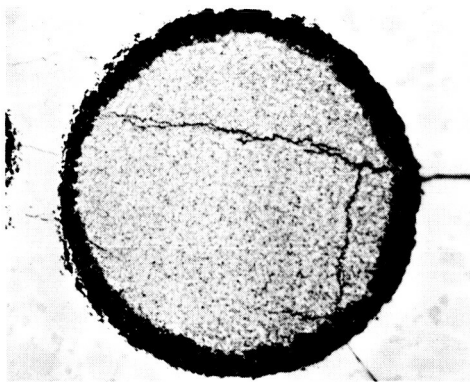
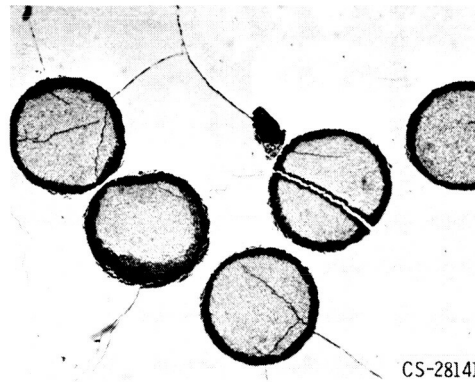


Figure 30. - Stress-rupture strengths for tungsten-fiber-reinforced copper composites as a function of volume percent fibers; continuous 5-mil-diameter tungsten fibers. Test temperature, 1500° F; helium atmosphere (ref. 14).

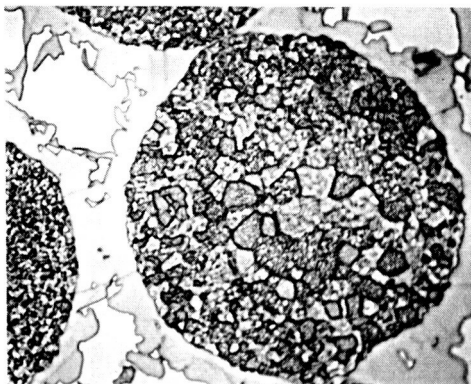


(A) X750.

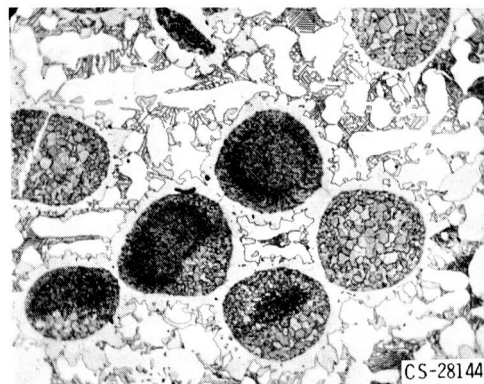


(B) X250.

Figure 31. - Tungsten fibers in columbium-nickel matrix; transverse section, as infiltrated (ref. 8).



(A) X750.



(B) X250.

Figure 32. - Tungsten fibers in cobalt base alloy (S-816) matrix; transverse section, as infiltrated (ref. 8).

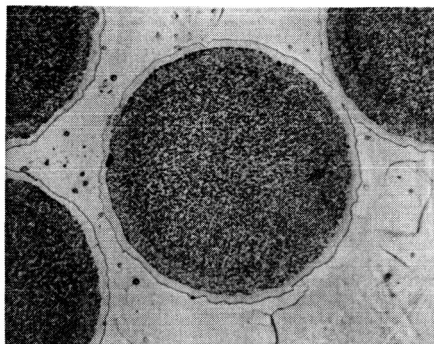


Figure 33. - Tungsten-fiber-reinforced nickel composite showing slight reaction zone with solid-state sintering.

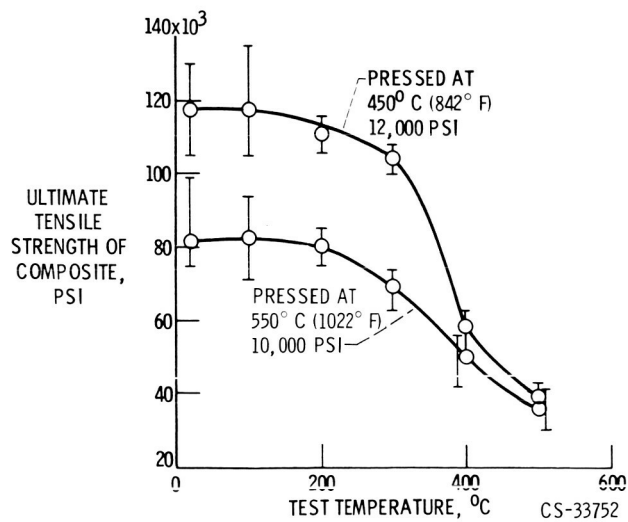


Figure 34. - Ultimate tensile strengths of silica-fiber-reinforced aluminum composites as a function of hot-pressing conditions and test temperatures; continuous silica fibers (ref. 16).

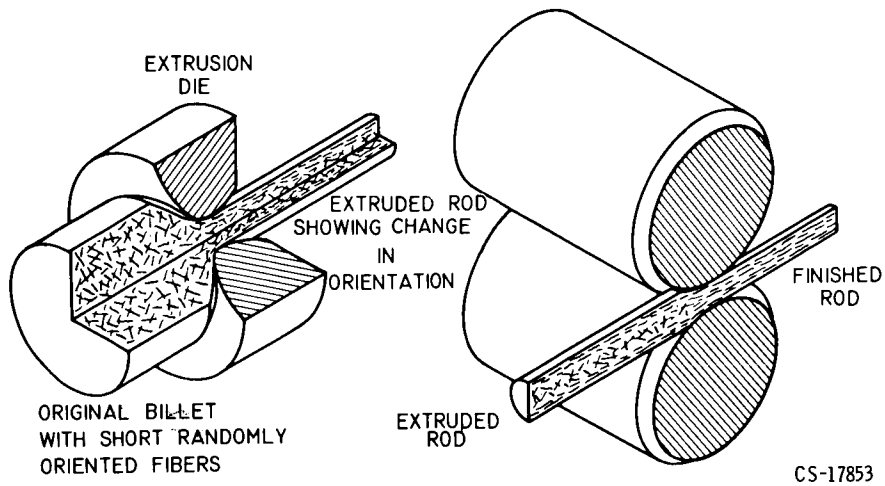


Figure 35. - Fabrication of fiber-reinforced metal matrix composites by extrusion and rolling; discontinuous fibers (ref. 17).

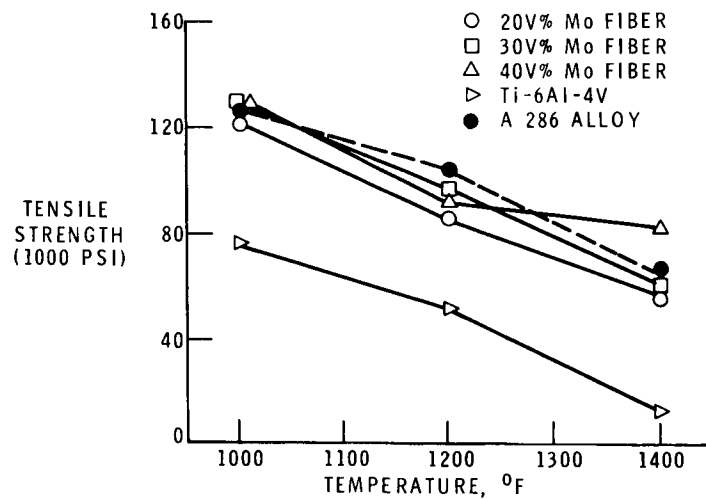


Figure 36. - Tensile strength versus temperature of molybdenum-fiber-reinforced Ti-6Al-4V alloy.

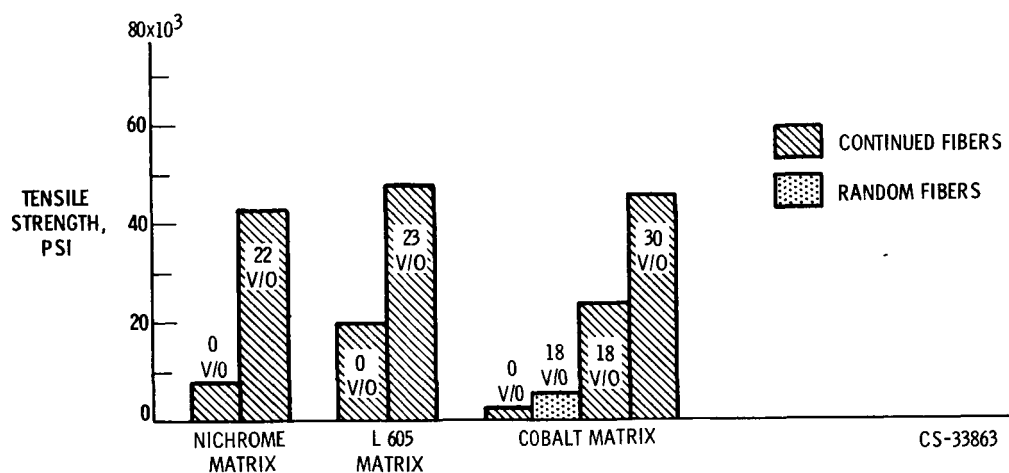


Figure 37. - High temperature tensile strengths of tungsten-fiber-reinforced cobalt or nickel base matrix composites; 10-mil-diameter tungsten fibers as-hot-pressed condition; test temperature, 2000° F (ref. 18).

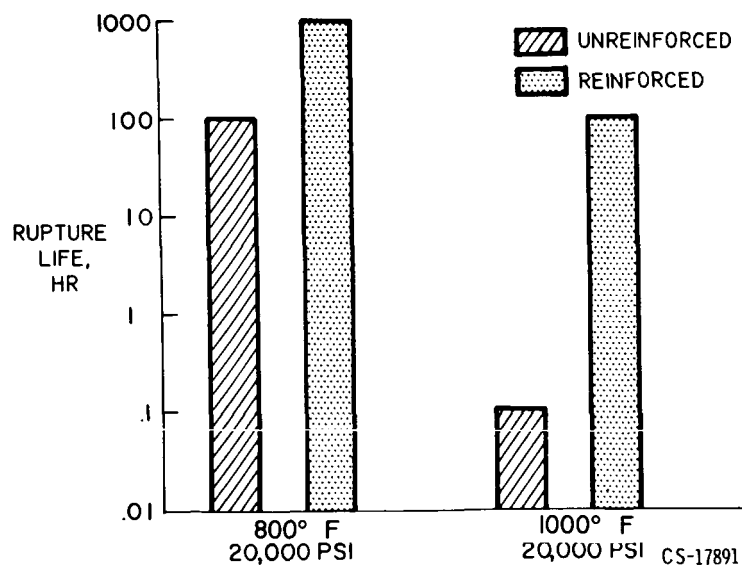


Figure 38. - Stress-rupture life of molybdenum-fiber-reinforced titanium matrix composites compared with unreinforced titanium, both as a function of test temperature; 10 volume percent fibers (ref. 17).

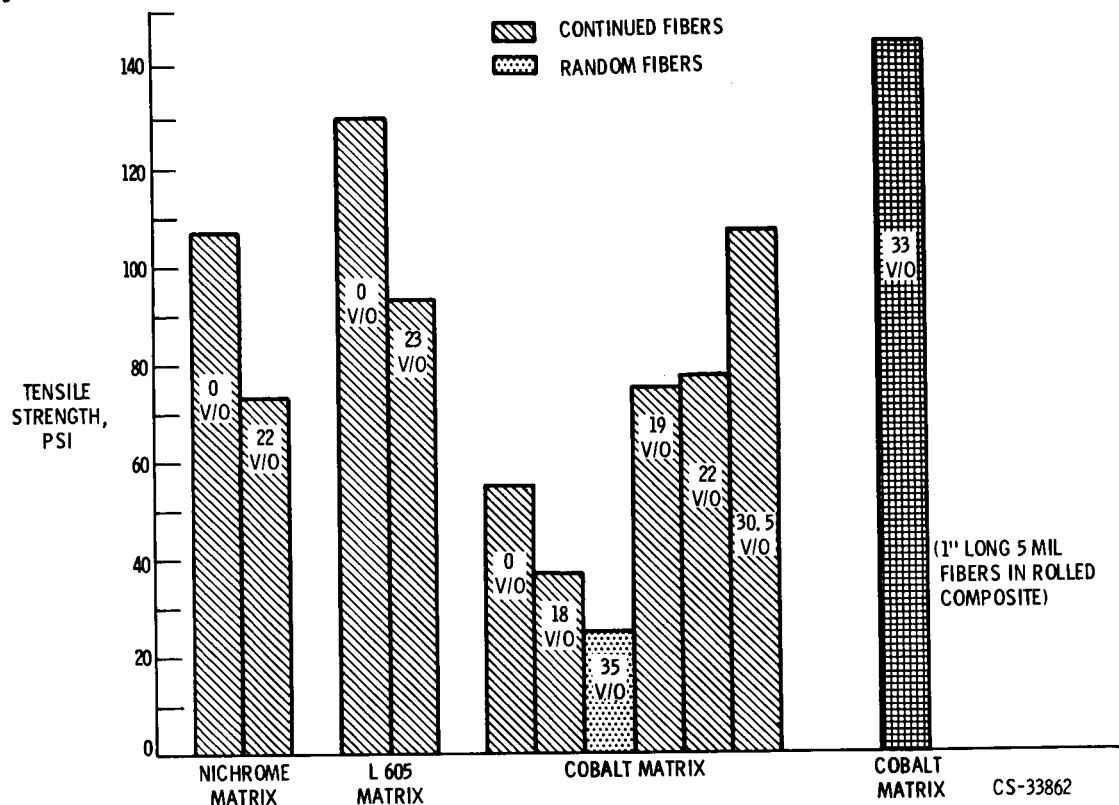
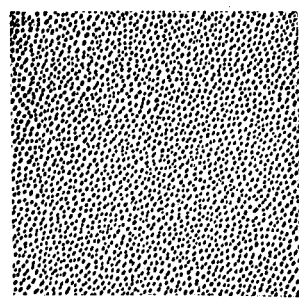
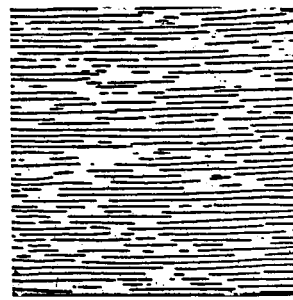


Figure 39. - Room temperature tensile strengths of tungsten-fiber-reinforced cobalt or nickel base matrix composites; discontinuous 5-and 10-mil-diameter tungsten fibers as-hot-pressed condition (ref. 18).



(a) Transverse section; growth direction; X500.



(b) Longitudinal section; growth direction, left to right; X200.

CS-28244

Figure 40. - Microstructure of unidirectionally solidified Al-Al<sub>3</sub>Ni eutectic specimen (ref. 19).



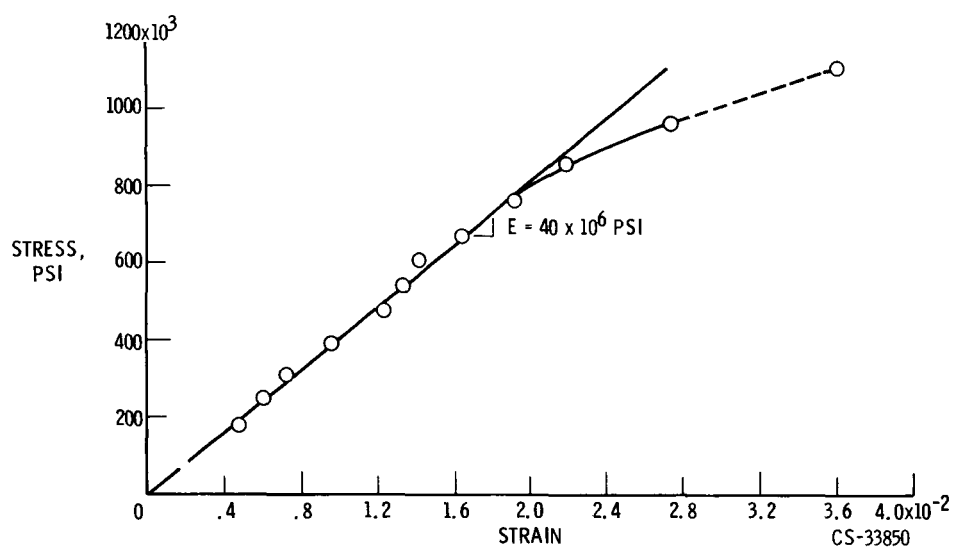
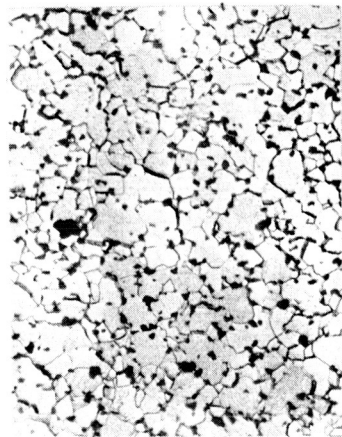


Figure 41. - Stress-strain curve for chromium whisker which was directionally solidified from copper-chromium alloy. Dimension, 0.45 micron; cross-sectional area, 0.159 square microns circular (ref. 19).



(A) UNREINFORCED TUNGSTEN,  
CROSS SECTION.



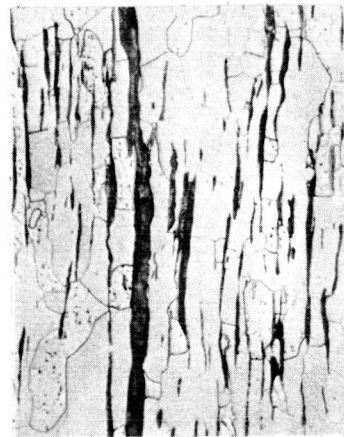
(B) TYPICAL CROSS SECTION,  
TUNGSTEN PLUS 8 V/O ZrO<sub>2</sub>.



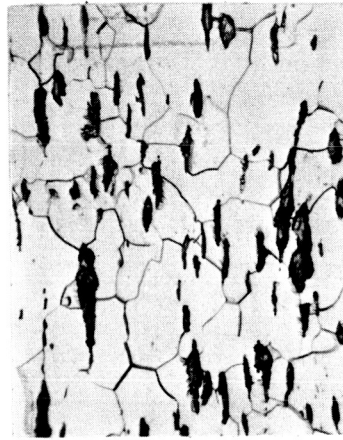
(C) TUNGSTEN PLUS 8 V/O ZrO<sub>2</sub>,  
LONGITUDINAL SECTION.



(D) TUNGSTEN PLUS 8 V/O Y<sub>2</sub>O<sub>3</sub>,  
LONGITUDINAL SECTION.



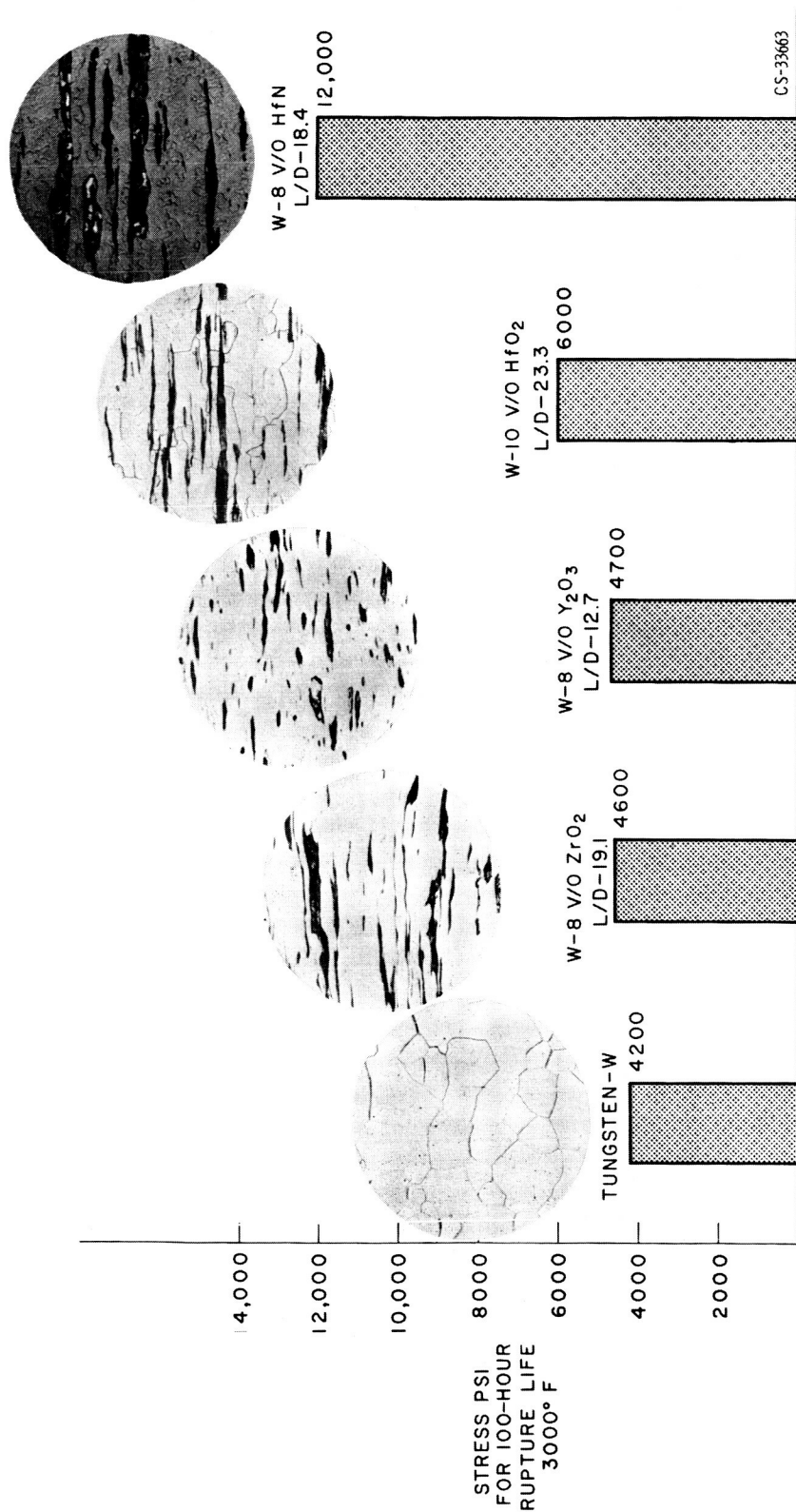
(E) TUNGSTEN PLUS 10 V/O HfO<sub>2</sub>,  
LONGITUDINAL SECTION.



(F) TUNGSTEN PLUS 8 V/O ThO<sub>2</sub>,  
LONGITUDINAL SECTION.

CS-32885

Figure 42. - Microstructures of extruded tungsten and tungsten composites containing "in situ" fibered refractory oxides (ref. 20); X500.



BILLET COMPOSITION AND FIBER LENGTH-TO-DIAMETER (L/D) RATIO

Figure 43. - Stress-rupture strength of fiber bearing tungsten base composite materials showing microstructures and giving length-to-diameter ratios of "in situ" formed fibers; test temperature, 3000° F (ref. 20); X500.

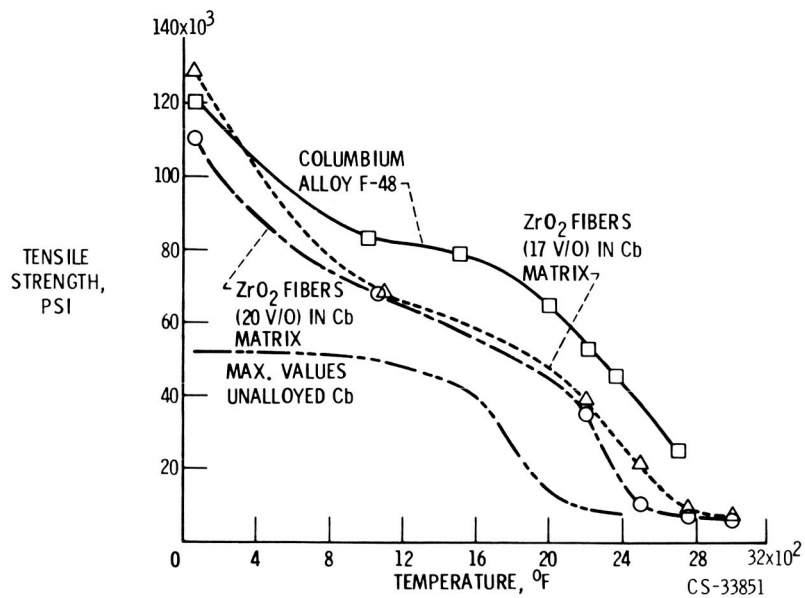


Figure 44. - Tensile strength of "in situ" extruded ZrO<sub>2</sub> ceramic-fiber-reinforced columbium matrix composites as a function of temperature (ref. 21).

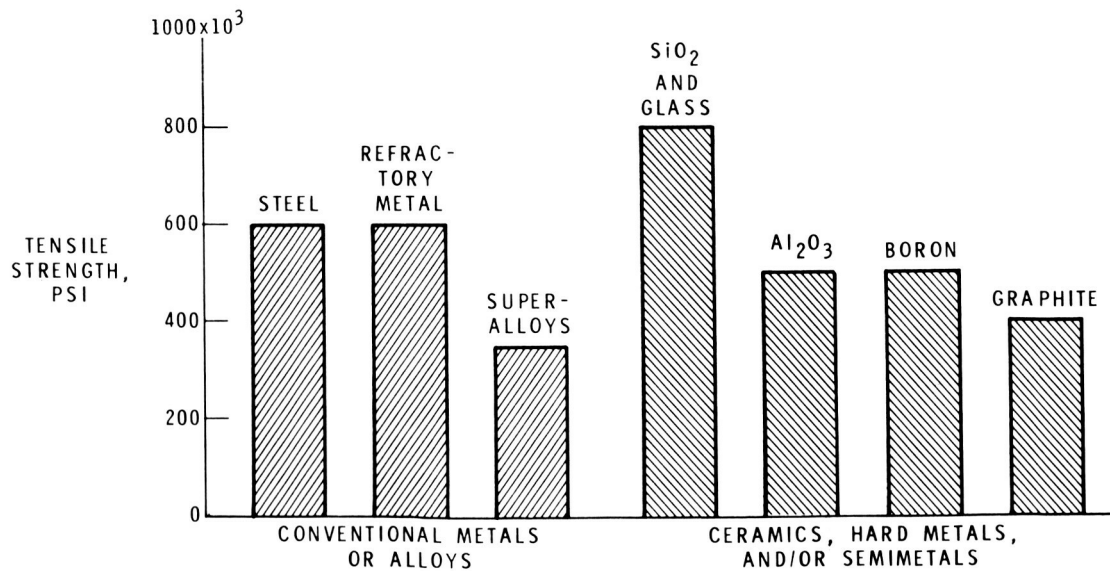


Figure 45. - Room temperature tensile strength of polycrystalline or glassy fibers.

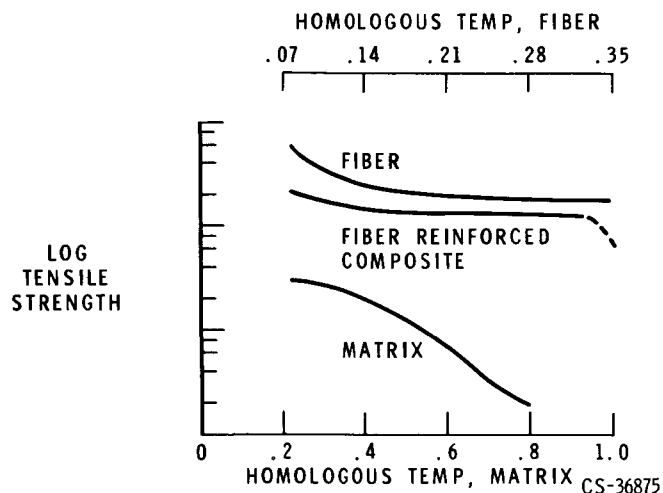


Figure 46. - Schematic comparison of tensile strength of composite and composite components as a function of homologous temperature.

- CALCULATED STRENGTHS OF DISPERSION STRENGTHENED Ni MATERIALS
- STRENGTHS OF FIBER COMPOSITES BELIEVED POSSIBLE
- SUPERALLOY STRENGTH ESTIMATES (25% ABOVE TODAY'S VALUES)
- CONSERVATIVE STRENGTH ESTIMATES FOR FIBER COMPOSITES
- SUPERALLOY STRENGTHS TODAY
- EXPECTED STRENGTHS OF DISPERSION STRENGTHENED MATERIALS
- DISPERSION STRENGTHENED Ni TODAY

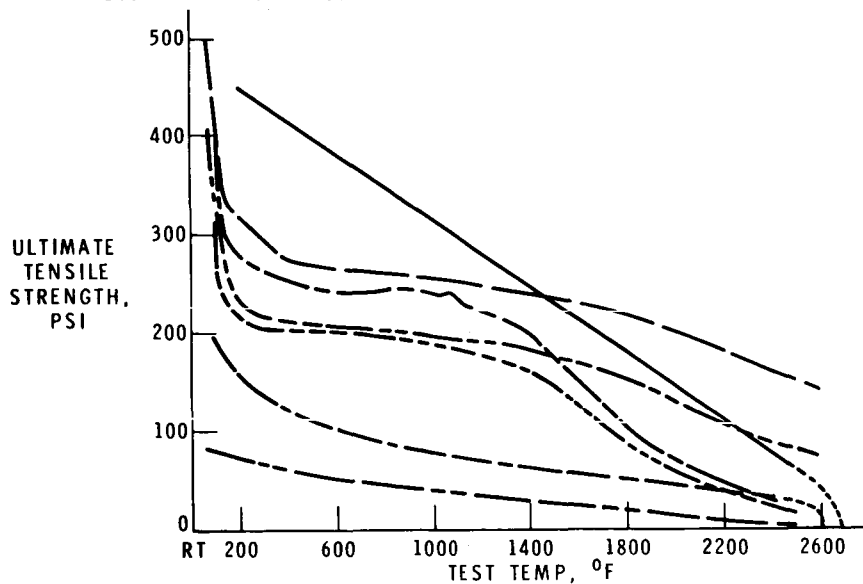


Figure 47. - Potential tensile strengths of fiber-superalloy composites, superalloys, and dispersion strengthened materials.

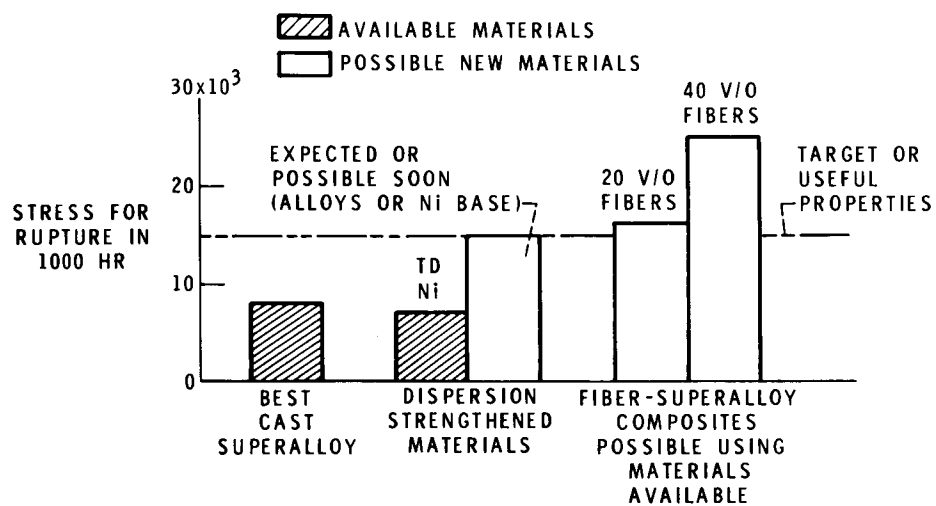


Figure 48. - Composites for stress-rupture applications possible in near future. Hypothetical target properties: 15,000 psi, 1000 hours, 2000° F.